COMPARATIVE ANALYSIS OF FLEXIBLE TRANSDUCERS

by

Antarjot Kaur
A Thesis
Submitted to the
Graduate Faculty
of
George Mason University
in Partial Fulfillment of
The Requirements for the Degree
of
Master of Science
Bioengineering

Committee:

_____ Dr. Parag Chitnis, Thesis Director

_____ Dr. Eugene Kim, Committee Chair

_____ Dr. Pilgyu Kang, Committee Member

_____ Dr. Avrama Blackwell, Department Chair

Date: 07/13/2023

Summer Semester 2023
George Mason University
Fairfax, VA

Comparative Analysis of Flexible Transducers

A Thesis submitted in partial fulfillment of the requirements for the degree of Master of Science at George Mason University

by

Antarjot Kaur
Bachelor of Science
George Mason University, 2021

Director: Parag Chitnis, Associate Professor
Department of Bioengineering

Summer Semester 2023
George Mason University
Fairfax, VA

DEDICATION

I would like to dedicate my thesis work to all a part of my journey. Thank you to my friends who have always pushed me to grow and take on new challenges. I would like to express gratitude to Derrick for his endless support and holding down the fort on my lowest days. I would also like to acknowledge my mentors Ahmed Bashatah, Alex Baker, Dr. Shani Ross, and Randy Warren for their invaluable insight, guidance, and endless support throughout my degree. I am grateful to all of those who have contributed to my journey.

ACKNOWLEDGEMENTS

I wish to thank my advisor, Dr. Parag Chitnis, for his guidance and support throughout this process. I also want to thank the members of my committee for their input: Dr. Parag Chitnis, Dr. Pilgyu Kang ,and Dr. Eugene Kim . Finally, thank you to the lab engineers Ahmed Bashatah and Alex Baker.

TABLE OF CONTENTS

LIST OF TABLES

LIST OF FIGURES

LIST OF EQUATIONS

LIST OF ABBREVIATIONS

Computer Aided Design ..... CAD
Fast Fourier Transform ..... FFT
Kilopascals ..... kPA
Motion mode ..... m-mode
Musculoskeletal Injuries ..... MSKI
Musculoskeletal Disorders ..... MSD
Polyethylene Terephthalate ..... PET
Polyimide ..... PI
Piezoelectric Micromachined Ultrasonic Transducer ..... PMUT
Polyvinylidene Fluoride ..... PVDF
Range of Motion ..... ROM
Region of Interest ..... ROI
Signal to Noise Ratio ..... SNR
Surface Electromyography ..... sEMG

ABSTRACT

COMPARATIVE ANALYSIS OF FLEXIBLE TRANSDUCERS

Antarjot Kaur, M.S.

George Mason University, 2024

Thesis Director: Parag Chitnis

In 2020 the private sector reported 247,620 musculoskeletal injuries because of day-to-day activities [1]. Musculoskeletal Injuries are a result of day-to-day activities and rarely evaluated in a timely manner. To understand musculoskeletal injuries, there lacks a clear, consistent, and repeatable method for capturing muscle function during dynamic tasks. Current methods of tracking and understanding muscle function include dynamometry, motion capture, and surface electromyography (sEMG) [2]. However, these methods are not ideal for examining musculoskeletal injuries for dynamic tasks.

To address the shortcomings of issues in tracking muscle function during dynamic tasks to better understand musculoskeletal injuries, the focus of this work will revolve around ultrasound transducers specifically, the methods to design, build, test, and compare with other flexible transducers. Characterizing methods include examining the signal frequency components, acoustic pressure produced by the transducer, and the imaging ability of the transducer. This thesis goes over the background and need for

flexible transducers, development and analysis of a flexible transducer, and a comparative analysis against other flexible transducers.

INTRODUCTION

MUSCULOSKELETAL DISORDERS PREVALENCE

Musculoskeletal disorders are prevalent in over 50% of the American population [3]. Musculoskeletal injuries (MSKIs) occur when any musculoskeletal structures, such as tendons, ligaments, muscles, joints, etc. are injured. MSKIs occur due to acute or a culmination of traumatic events to the musculoskeletal structures [4]. Identifying a MSKI early can minimize the severity or even prevent the development of MSDs [5]. To identify the presence and impact of an MSKI, biofeedback (i.e., Electromyography, Force, Range of Movement) from the muscle must be obtained during the excitation of the muscle of interest [6][7]. Evaluating musculoskeletal injury through employing a diverse set of range of movement (ROM) tasks can be done using ultrasound as it is an imaging modality that can examine musculoskeletal structures and is available in portable form factors [8][9].

Dynamometry and surface Electromyography (sEMG) are other methods of tracking muscle function that are limited. Dynamometry generates information about a force applied over an area but lacks the ability to isolate the specific muscles and force applied by the muscles without a level of assumptions and back calculations [10]. sEMG tracks muscle function by receiving electrical signals through the skin from contracting muscle fibers to electrodes attached to the arm [11]. Skin condition, electrode placement,

and muscle movement must be taken into consideration as any of these factors can impact the transmission and Signal-Noise-Ratio (SNR) of received electrical signals from contracting muscle fibers. In situations where sEMG is used to evaluate muscle function, sEMG is limited to observing superficial muscle activity, inaccuracies due to muscle-cross talk, and low signal-to-noise-ratio (SNR) [12]. Dynamometry and sEMG are not tools utilized in the clinical workflow. Ultrasound is embedded into the clinical workflow and can be used to visualize musculoskeletal structures [13][14]. However, there are limitations of ultrasound transducers used during movement that impact the stability of the transducer on the region of interest (ROI). Instability of the transducer results in angling during dynamic tasks that can create issues in imaging the ROI including motion artifact, depth penetration, limited field of view, and operator dependency [15]. Also attempting to stabilize the transducer with a strap or holder could possibly compress the muscle and limit ability to observe and understand the muscle function during a dynamic task. To mitigate the issue of instability during the performance of dynamic tasks, there has been development of flexible transducers.

FLEXIBLE TRANSDUCERS

Current research in flexible transducers includes Piezoelectric Micromachined Ultrasonic Transducer (PMUT), Polymers with embedded piezoelectric ceramics, and organic piezoelectric films [16].

PMUTs are transducers that utilize piezoelectric films and micromachining techniques to produce a small, scaled transducer. PMUTS are easily integrable into

electronic systems and are broad-band devices. However, PMUTS are costly due to their fabrication process and materials and inconsistency in reproduction [16]-[18].

Polymers with embedded piezoelectric ceramics are flexible polymers that contain piezoelectric ceramics. The goal of polymers with embedded piezoelectric ceramics is to reduce fragility and to increase conformability. However, there is only a minute improvement in fragility and conformability of piezoelectric ceramics embedded into polymers compared to isolated piezoelectric ceramics that still limits the conformability of the piezoelectric ceramics embedded into polymers to the ROI [16]-[19].

Piezoelectric films are thin flexible films with piezoelectric properties that can be made biocompatible, conformable, and are economical. When considering, conformability, cost, and safety for tracking dynamic muscle function and diagnostics of MSIs, a piezoelectric film is the most ideal due to material flexibility, biocompatibility, piezoelectric properties, and economical nature [16][18]-[20].

Piezoelectric Film transducers

Piezoelectric film-based transducers are piezoelectric materials interposed between a positive and ground electrode (**Figure 1**). When excited by voltage applied across the device, the piezoelectric material deforms to allow conversion between electrical and mechanical energy as acoustic waves [21][22].

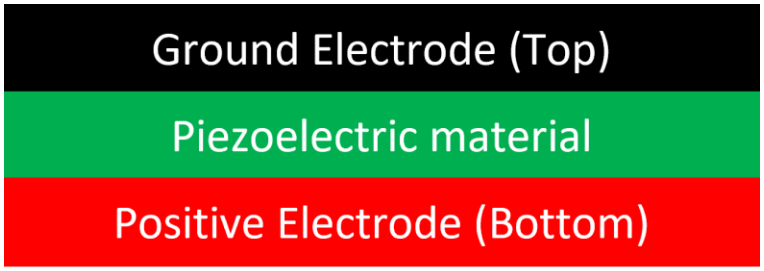

Figure 1: A basic schematic of a transducer where a piezoelectric material is interposed between a ground and positive electrode.

Optimal choice of a piezoelectric material for a transducer is governed by the desired SNR and resolution of pulse-echo signals from tissue interfaces [23]. Polyvinylidene Fluoride (PVDF) is a piezoelectric flexible polymer that is used for flexible transducers [24]. To determine if a piezoelectric material used in the fabrication of an ultrasound transducer is appropriate for the application of diagnosing musculoskeletal disorders, it is important to characterize the signal frequency components and acoustic pressure produced by the transducer.

CHARACTERIZING TRANSDUCERS

When characterizing a transducer, key factors to consider are the signal frequency components, acoustic pressure, and the ability to image through tissue . Frequency response and bandwidth of the signal are important to understand as the penetration depth and resolution of the signal produced by the transducer are frequency dependent [25]. Below is **Eq 1** that shows the wavelength λ is inversely proportional to the center frequency, f [26].

$$\lambda \approx c / f \qquad \text{(Eq 1)}$$

The Bandwidth is also inversely proportional as shown below in **Eq 3** [26][27]**.**

$$\text{BW} \approx f_{max} - f_{min} \quad \text{(Eq 2)}$$

$$\text{BW} \approx \frac{c}{\lambda_{max}} - \frac{c}{\lambda_{min}} \quad \text{(Eq 3)}$$

A shorter wavelength results in better axial resolution but attenuates faster and does not have deep penetration [27][28]. The longer the wavelength, the signal penetration depth increases, but axial resolution is sacrificed [27][28]. The signal frequency components, center frequency and bandwidth, can be used to understand the penetration depth and axial resolution.

Frequency response and usability can be determined using pulse-echo testing. The beam profile is characterized through hydrophone testing. Understanding the beam profile homogeneity and the pressure produced by the transducer is necessary to understand the strength and direction of the signal [25]. Along with the understanding of the signal frequency components and acoustic pressure of transducer, understanding the transducer's imaging capabilities during movement is important. Thus, taking m-modes using the transducer to observe the signal depth is important [26]. Based on these three forms of characterization, literature suggests a minimum requirement for imaging musculoskeletal structures with a frequency between 2 to 6 MHz [27][28]. This is because common musculoskeletal injuries occur in the leg, thighs, knees, and hips that require deeper penetration depth [29][30][31]. Since the injuries in 4 MHz transducer with a Bandwidth of 2 MHz would be a good trade-off between penetration depth and resolution [32]-[35].

Pulse-Echo

In an ultrasound system that uses pulse-echo, an electrical pulse is sent from a pulser-receiver to a transducer. The transducer contains a material that is piezoelectric, and the electrical signal is applied across the piezoelectric material interposed between two electrodes. When excited by the electrical pulse, the piezoelectric material vibrates, and acoustic waves propagate from the transducer through a medium [35]. The transducer receives and translates the reflected acoustic energy into electrical energy that is then stored and processed **(Figure 2)**.

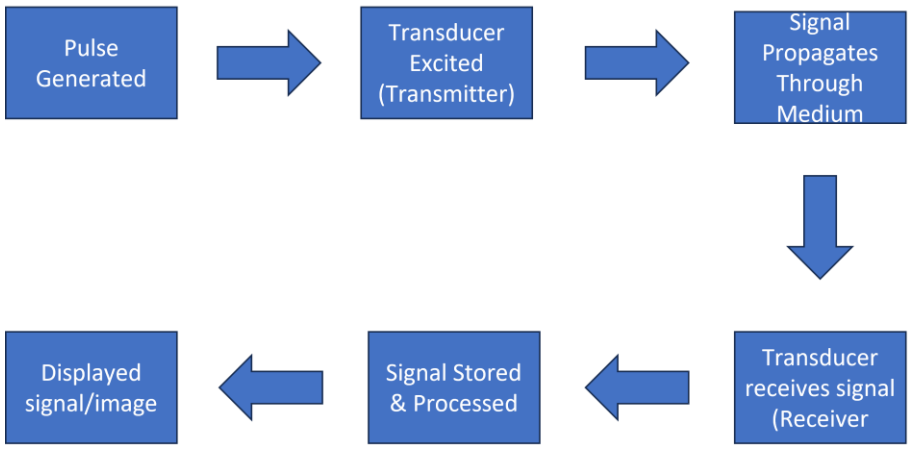

Figure 2: A diagram of the pulse-echo principal in ultrasound

A one-dimensional signal is received by the transducer observing the amplitude of the signal (voltage) over time, also known in ultrasound as acquiring an A-mode scan. In ultrasound, an A-mode scan is used to understand the signal strength, thickness of a material, and distance between different materials [36]. Applying a Fourier transform to

the same signal allows translation of the signal from the time domain to the frequency domain to understand key signal frequency components of the transducer related to the transducer's imaging capabilities[37].

Pulse-echo testing allows understanding of signal frequency components, but understanding the acoustic pressure profile of the transducer is also important to ensure proper signal propagation through confirming homogeneity of pressure across the cross-section and the entire distance of the beam profile. The next section will discuss how information about the pressure profile is acquired and interpreted through hydrophone testing.

Hydrophone

A hydrophone is an instrument used to characterize the acoustic pressure of a transducer with the environment being water. In hydrophone testing, the transducer acts as the signal transmitter and the hydrophone is the signal receiver [38][39]. An electrical signal is first applied to a transducer to excite the transducer. The acoustic waves produced by the transducer then propagate through water and are received by the hydrophone. The hydrophone scans each point across the face of the transducer and the expected beam of the transducer to produce 2D pressure maps of the cross-sectional and axial view of acoustic pressure profile in kilopascals (kPA) [40][41]. The acoustic pressure profile provides information on the direction the acoustic signal propagates, the penetration depth of the signal, and the homogeneity of the beam profile across the surface of the transducer and the distance the signal propagates (**Figure 3**). Utilizing the hydrophone to understand the acoustic pressure profile is important because it impacts

the resolution, image formation, safety, and beamforming in multi-elemental transducer arrays.

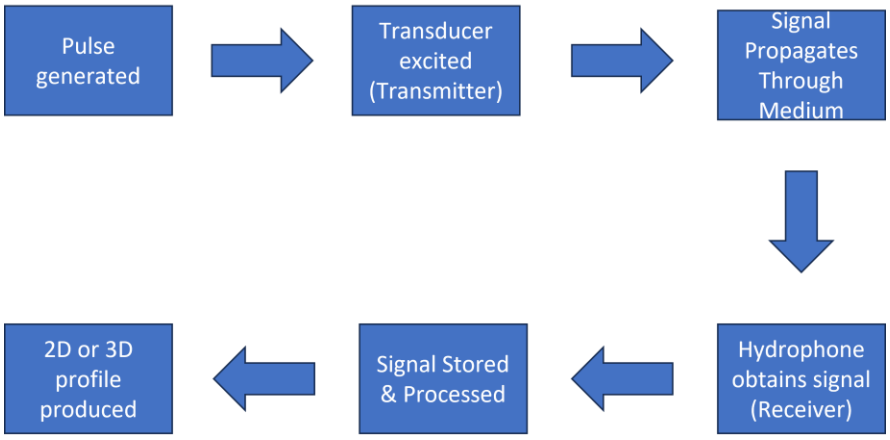

Figure 3: A diagram of the hydrophone testing

Imaging

When a region of interest (ROI) is observed over time during ultrasound data acquisition, this image is known as an m-mode scan [42]-[44]. As a signal is transmitted from a transducer, each time the signal reaches the acoustic boundary between two mediums, energy from the acoustic wave is reflected to the transducer due to acoustic impedance mismatch between the materials [45]. The m-mode scan is shown below in grayscale where the x-axis is time and the y-axis is the depth.

The white pixels correspond to areas that have a high acoustic impedance mismatch and black pixels correspond to low acoustic impedance differences. Acoustic impedance is high when reaching the boundary of two different tissue types [46]. Thus,

anatomical structures are identifiable as the change in tissue type will appear in the image. When a muscle is compressed or flexed, the distance of reflections from each anatomical structure relative to the transducer interface changes [47][48]. The change in distance between the transducer and the interface of the anatomical structure over time is trackable through acquisition of m-modes. Since musculoskeletal structures do compress or flex during a dynamic task and can be imaged through ultrasound, ultrasound is ideal for understanding muscle function during dynamic tasks.

PROJECT AND PAPER OVERVIEW

The goal of this project was to fabricate, characterize, and compare fabricated flexible transducers. The purpose behind fabricating and characterizing the transducer is to determine if the approach would be viable for imaging musculoskeletal injuries. Comparison between three fabrication strategies is done to determine and move forward with an optimal fabrication process for flexible transducers. The goal of this research will review several factors in fabricating the flexible piezoelectric transducer, a comparative analysis between the piezoelectric transducer fabricated against two other alternatives and the standard piezoelectric composites used in the field of ultrasound. These transducers will be compared using the above-mentioned characterization methods of pulse-echo, hydrophone testing, and imaging to understand the signal strength, functionality, acoustic pressure, and image quality. Understanding each transducer fabrication method and their effectiveness as well shortcoming as a transducer will add information to the field of flexible transducers used to assess musculoskeletal conditions during dynamic tasks.

SINGLE-ELEMENT TRANSDUCER

In fabricating a flexible multi-elemental transducer, it is important to break-down the problem to ensure optimized and reproducible fabrication and characterization methods of a transducer. Also, for several applications a single-element transducer is desired for wearable systems. The focus of this paper will be fabrication and characterization of a one-element transducer.

FABRICATION OF A ONE-ELEMENT TRANSDUCER

The flexible one-element transducer has a simple design of three layers shown below (**Figure 4**).

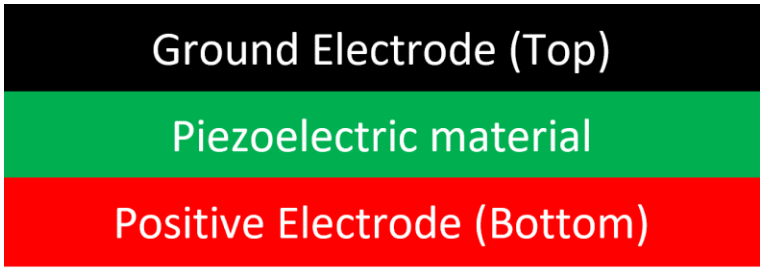

Figure 4: A basic schematic of a transducer where a piezoelectric material is interposed between a ground and positive electrode.

The bottom layer is a positive electrode made of a proprietary conductive ink printed by a 3D circuit board printer (Voltera) [49]. The active element area is a circle with a 7 mm

diameter. The active element is connected by an interconnect to a contact pad that connects to the excitation source (**Figure 5**).

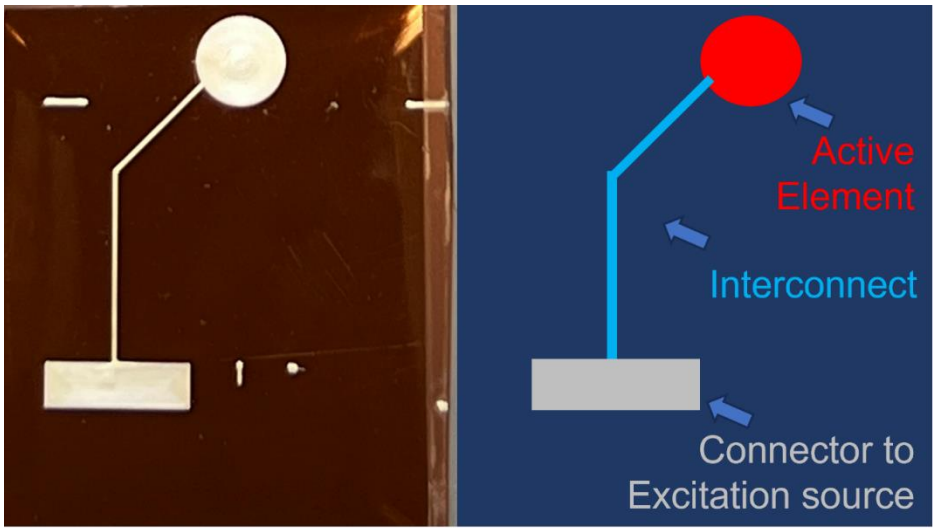

Figure 5: A basic schematic of the positive electrode of the transducer(right). The active element is a 7mm circle(red) connected by the interconnect(blue) to the contact pad(grey) where the excitation source will connect. The real device is shown on the left.

A piezoelectric film with a ground silver electrode on top is then adhered to the positive electrode with a 2-part adhesive known as Hysol [50]. A Polyethylene Terephthalate (PET) substrate is adhered over the positive interconnect to act as barrier between the two electrodes to prevent shorting [51][52]. Shorting between the positive and ground electrodes can happen due to ultrasound requiring direct contact between the transducer and a coupling medium such as gel or water. Thus, to prevent shorting, a PET substrate is added as a passivation layer over the positive electrode interconnect. The ground electrode on the piezoelectric material is extended by an interconnect on top of the PET substrate to a contact pad (**Figure 6**).

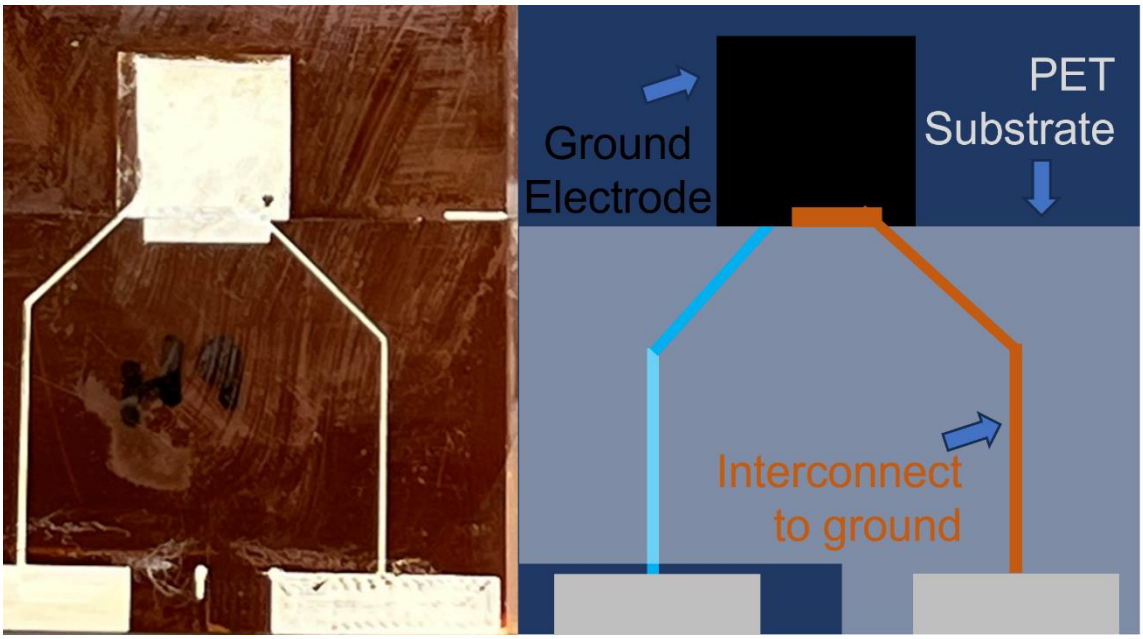

Figure 6: A basic schematic of the ground electrode of the transducer (right). The ground electrode(black) is already screen printed by the manufacturer on top of the PVDF layer and is connected by the interconnect(orange) to the contact pad(grey) where the ground source will connect. The real device is shown on the left.

When optimizing fabrication of the devices, the Hysol thickness and piezoelectric thickness were two parameters that impacted the performance of the transducer. Hysol was chosen as it is known to bond materials with minimal amounts, disperses evenly and easily due to its low-viscosity and ensures contact and minimal air gaps. The thickness of the piezoelectric can change the frequency response of the transducer and the penetration depth. Thus, two parametric experiments were performed with differing Hysol levels and differing PVDF film thicknesses to understand the optimal parameters for fabrication of the flexible transducer.

PARAMETRIC EXPERIMENTS

Hysol Experiments

Contact between the piezoelectric material and two electrodes is imperative for transmission of the acoustic signal. Enough adhesive needs to be applied to mitigate air gaps between the piezoelectric material for signal transmission. Excessive amounts of adhesive can impede the movement of the flexible piezoelectric material once cured. Impairment to the piezoelectric material's signal directly impacts the frequency components of the signal, acoustic pressure of the device, and imaging quality of the transducer.

When understanding the impact of the Hysol added between layers of the device, it is important to have a baseline expectation of the piezoelectric film's frequency components. One component that can be easily calculated is the center frequency of a piezoelectric material. A transducer's piezoelectric center frequency (f) can be calculated by knowing the thickness (d) and speed of sound (v) based on the equation below (**Eq 4**) [39].

$$f = \frac{v}{2d} \qquad \text{(Eq 4)}$$

If a piezoelectric material has only two electrodes, the piezoelectric material functions close to center frequency. The piezoelectric material used for the parametric experiment with different levels of Hysol is a 100 μm thick PVDF film with screen printed silver electrodes purchased from PolyK. A speed of sound for the PVDF was provided by the

manufacturer at 2,200 m/s and a thickness of 100 μm. Thus, the expected center frequency calculated from **Eq 4** of the PVDF film with screen printed electrodes is 11 MHz. Before adhering the piezoelectric material to the positive Voltera electrode, the screen-printed positive electrode applied by the manufacturer was swabbed with acetone and completely removed. The PVDF film was then adhered to the Voltera ink electrode. Nine devices in total were tested that had a Hysol level of 1 μL, 2 μL, or 5 μL. The purpose of testing the varying levels of Hysol were to ensure good adhesion and observe any impact of the Hysol on the device performance. The devices were then characterized through pulse-echo, hydrophone, and image testing.

Hysol Deposition

Devices were fabricated with a 100 μm thick PVDF film and adhered to the positive electrode with either 1 μL, 2 μL, or 5 μL of Hysol. Using a micropipette, the Hysol was deposited on the center of the PVDF and adhered to the active element of the positive electrode. A glass slide and 200 g weight were placed on top of the device sequentially (**Figure 7**).

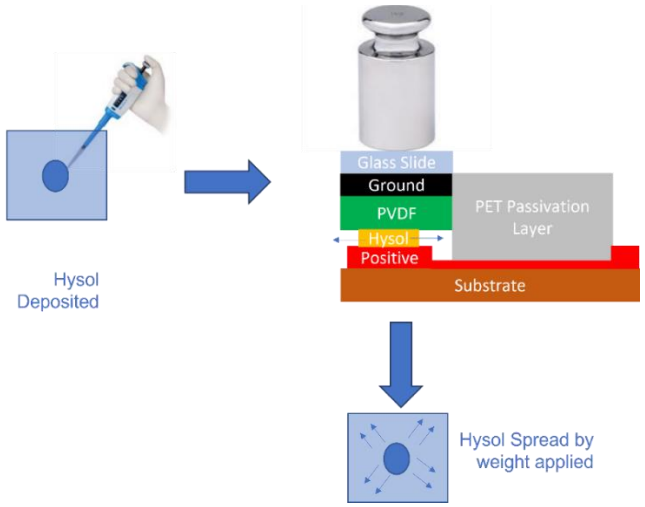

Figure 7: A basic schematic Hysol deposition and spreading. The Hysol is deposited using a micropipette in the center of the PVDF (Top left). A glass slide and 200 g weight are put on top of device to help the Hysol spread evenly (Right).

The devices were in the oven for 8 hours at 50 C to cure the Hysol. Some devices were damaged during the fabrication process due to poor or excessive bonding. Poor bonding was due uneven spreading of Hysol for devices with insufficient amounts of Hysol. Excessive adhesion was due to an excess of Hysol leaking and bonding the glass slide with the top electrode. In the case of excessive adhesion, once the Hysol was cured, either the top electrode or the entire PVDF film would adhere to the glass slide. The devices undamaged were then tested through acoustic testing, hydrophone testing, and m-mode testing (**Figure 8**).

Figure 8: Above are the end results after fabrication using 1 µL, 2 µL, or 5 µL of Hysol. 1 µL kept the piezoelectric film adhered to the electrode (left). The 2 µL devices had fabrication issues when the Hysol would leak out from under and create a layer of adhesion between the top electrode and glass slide (center) . The 5 µL Hysol devices had similar failures to the 2 µL devices, but the PVDF came off of the bottom electrode (Right).

The devices undamaged were then tested through acoustic testing, hydrophone testing, and m-mode testing.

Acoustic Testing

For acoustic testing, he set-up was comprised of a pulser-receiver (OLYMPUS 5073PR Pulser Receiver), a connector for the transducer, and an oscilloscope (LeCroy LT344L) as seen below **(Figure 9)**. Acoustic tests were done with a gel-pad medium and pulser-receiver for excitation of the transducer. The device was laid flat with the ground electrode side of the transducer in contact with the gel-pad (**Figure 9**).

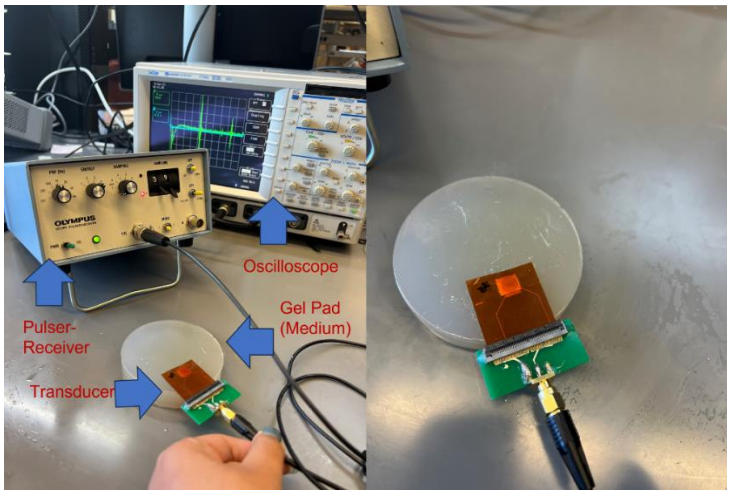

Figure 9: Above is the set-up of the pulse-echo testing(left) and the placement of the transducer on the gel-pad.

Optimal parameters for the pulser-receiver were chosen to amplify the signal and remove noise (**Table 1**). The pulse repetition frequency(PRF) is the frequency of the pulses emitted from the pulser-receiver to the transducer. The energy refers to the energy of the transmitted pulse and the highest energy was chosen as PVDF transmitting abilities are weaker than standard piezoceramics. The damping was chosen at the lowest setting of 12 ohms as the signal received is weak. The maximum gain available was chosen to amplify the signal to observe the signal. When applying a high gain, the signal noise was amplified. Thus, the low-pass filter on the pulser-receiver was used to reduce the noise.

Table 1: Above are the settings of the pulser-receiver for the pulse-echo tests of the transducer on the gel-pad.

Pulse-Echo Setting	Setting Value
PRF	1000 Hz
Energy	4 (16 μ J)
Damping	1 (12 Ohms)
Gain	39 dB
High Pass Filter	OFF
Low Pass Filter	ON

The low pass filter was always applied to remove low frequency noise. The pulser-receiver was connected to the oscilloscope as the oscilloscope is a tool used to pictographically display the time-variant signal from the transducer. Based on the thickness of the gel pad and the speed of sound, we can validate that the signal acquired is the signal expected **(Eq 6)**.

$$\text{Distance} = (v * t) / 2 \qquad \text{(Eq 5)}$$

$$\text{Gel Pad thickness} = (\text{gelpad speed of sound} * \text{time of flight}) / 2 \qquad \text{(Eq 6)}$$

The estimated speed of sound is 1540 m/s with a thickness of 2 cm. The estimated time was 26.02 μs and the time of the signal to be transmitted was approximately the same. Once the signal was received and stored. The received signal was then recorded and stored on a computer. MATLAB was used to process the signal by taking the Fast

Fourier Transform (FFT) to obtain the frequency components of the signal. This allowed observation of the signal in the frequency domain and acquire metrics such as the center frequency and bandwidth of the signal.

The table below shows the testing for frequency components of the devices with 1 µL, 2 µL, or 5 µL of Hysol for Pulse-echo testing (**Table 2, Table 3, Table 4**).

Table 2: This is a table for the devices with 1 µL of Hysol

Device Name	Pulse-echo Amplitude	Center Frequency	Bandwidth
Mic1_Device 1	0.4 V	3.42 MHz	1.89 MHz
Mic1_Device 2	1.2 V	3.78 MHz	2.11 MHz
Mic1_Device 3	1 V	7.83 MHz	3.42 MHz
Mic1_Device 4	0.9 V	6.85 MHz	4.89 MHz
Mic1_Device 5	0.4 V	3.43 MHz	5.87 MHz

Table 3: This is a table for the devices with 2 µL of Hysol

Device Name	Pulse-echo Amplitude	Center Frequency	Bandwidth
Mic2_Device 1	0.9 V	7.34 MHz	2.25 MHz
Mic2_Device 2	0.45 V	3.66 MHz	1.90 MHz

Table 4: This is a table for the devices with 5 µL of Hysol

Device Name	Pulse-echo Amplitude	Center Frequency	Bandwidth
Mic5_Device 1	0.4 V	3.66 MHz	1.61 MHz
Mic5_Device 2	0.9 V	4.21 MHz	2.44 MHz

The tables above have been translated into graphs below to observe trends between devices with Hysol levels of either 1 µL, 2 µL, or 5 µL. The two observations when interpreting the results for the pulse-echo tests were the change in bandwidth and center frequency due to the different levels of Hysol. When comparing the center frequency between the devices with different Hysol levels, there was a decrease in center frequency as the Hysol amount increased (**Figure 10**). The bandwidth was also reduced as the Hysol amount was increased (**Figure 11**). The primary reason for focusing on these two frequency components is because the center frequency impacts the penetration depth of the image and the bandwidth impacts the resolution of the image in ultrasound. The ideal center frequency is a 4MHz transducer with a Bandwidth of 2 MHz. The Hysol amount that gives a center frequency close to the desired 4MHz and a bandwidth of 2 MHz is 5 µL of Hysol.

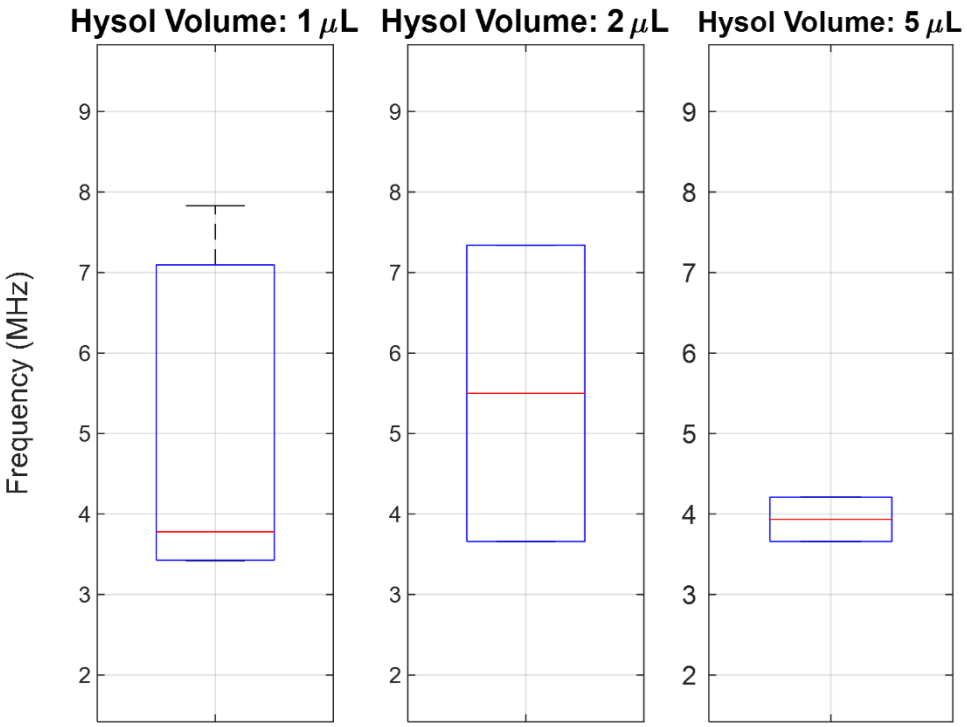

Figure 10: A decrease in center frequency as Hysol amount increases. This was taken from pulse-echo testing

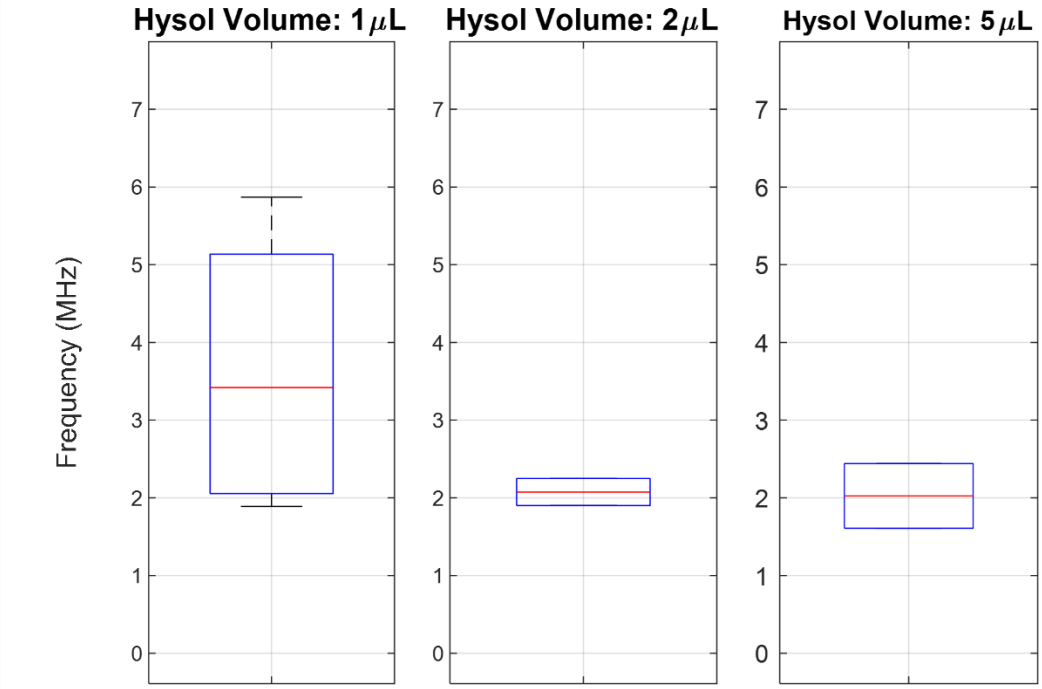

Figure 11: Center frequency decreases as Hysol amount increases. This was taken from pulse-echo testing data.

Hydrophone

The data collected from the hydrophone scanning across the flexible transducer to provide the pressures from the axial view and cross-sectional view of the transducer's beam profile. To obtain the data for the cross-sectional view, the hydrophone scanned across the device to produce a 20 x 20-point grid. To obtain the data collected for the axial view, the hydrophone scanned across the device to output a 21 x 16 grid. The data collected from the hydrophone can be converted to pressure to view the beam profile and cross-sectional view in kilopascals(kPA) as two 2D-grids (**Figure 12).**

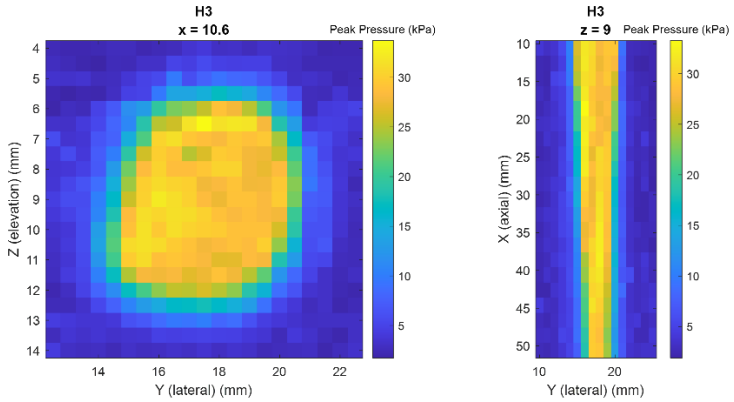

Figure 12: The cross-sectional and beam view of the beam produced by device H3.

Table 5: This is a table for the devices with 1 µL of Hysol

Device Name	Signal Amplitude	Center Frequency	Bandwidth
Mic1_Device 1	0.12 V	3.91 MHz	5.69 MHz
Mic1_Device 2	0.12 V	3.05 MHz	3.27 MHz
Mic1_Device 3	0.20 V	4.81 MHz	6.35 MHz

Table 6: This is a table for the devices with 2 µL of Hysol

Device Name	Signal Amplitude	Center Frequency	Bandwidth
Mic2_Device 1	0.04 V	6.59 MHz	1.59 MHz
Mic2_Device 2	0.05 V	3.17 MHz	2.66 MHz

Table 7: This is a table for the devices with 5 µL of Hysol

Device Name	Signal Amplitude	Center Frequency	Bandwidth
Mic5_Device 1	0.05 V	5.74 MHz	1.50 MHz
Mic5_Device 2	0.06 V	3.66 MHz	2.05 MHz

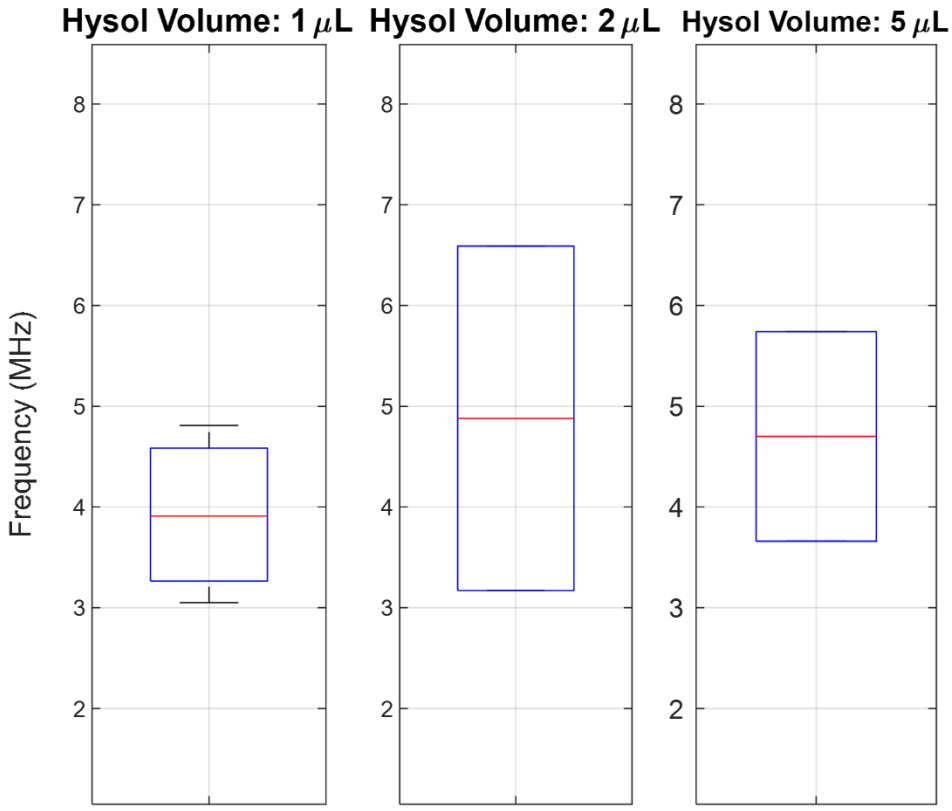

Figure 13: This is a graph showing the slight downward trend as Hysol levels increase, center frequencies decrease.

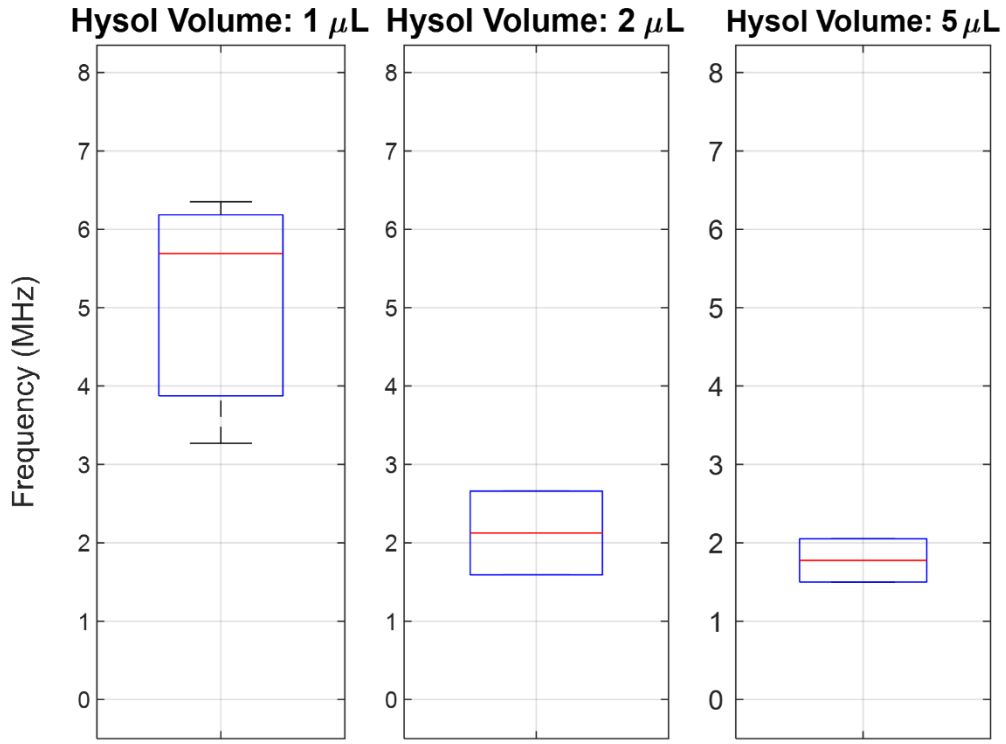

Figure 14: This is a graph showing the slight downward trend as Hysol levels increase, Bandwidths decrease.

From the data above there are three observations of change in center frequency, change in bandwidth, comparison to standardized frequency metrics for application, and comparison to center frequency and bandwidth of pulse-echo measurements. For the hydrophone, the center-frequency seems to increase slightly as Hysol amount is increased **(Figure 13)**. The Bandwidth of the device decreases as the Hysol amount increases (**Figure 14)**. The 5 μL Hysol devices have the center frequency and the bandwidth closest to the desired center frequency of 4 MHz and 2 MHz bandwidth. When

comparing the Center Frequency and Bandwidth tests between both the Pulse-echo and Hydrophone tests, the devices for the 1 µL, 2 µL, 5 µL, 66% of the devices had similar results. There is an expectation of a small variance in bandwidth and center frequency from hydrophone data vs pulse-echo data. Variance can occur because in pulse-echo the device is both the transmitter and receiver, but in hydrophone testing the device is a transmitter and the hydrophone is the receiver of the signal. Thus, some variability is expected. When observing the cross-section of the Beam profile for all three Hysol levels, the homogeneity of the beam profile improves as more Hysol is added.

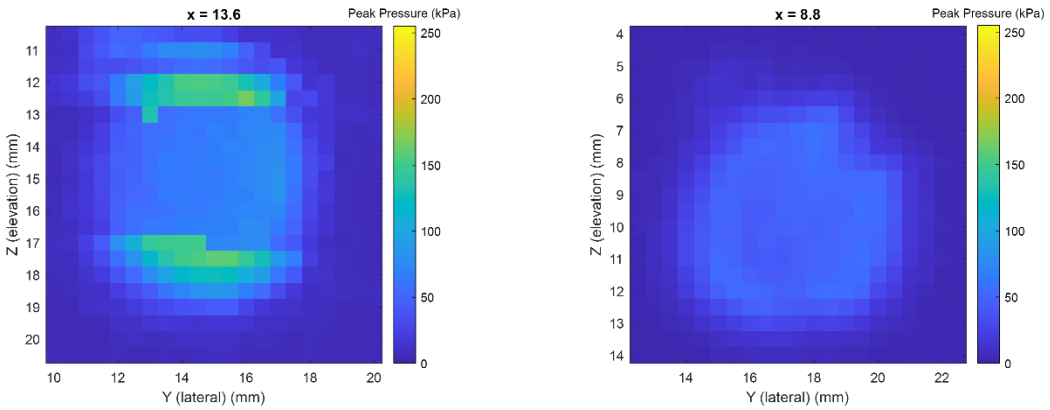

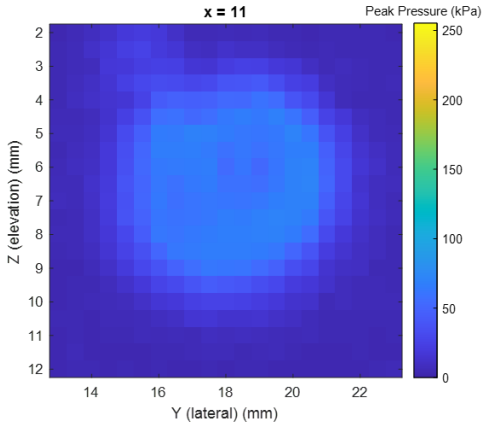

Figure 15: From left to right: 1 µL of Hysol, 2 µL of Hysol, 5 µL of Hysol. As the Hysol levels increase the homogenity of the cross-section increases.

However, the peak pressure for the 1 µL devices averaged across has a stronger peak pressure than the 2 µL and 5 µL devices. Also, over adhesion was common for both the 2 µL and 5 µL devices (**Figure 15)**. Thus, many were damaged in the fabrication process (**Figure 16**).

Figure 16: Above are the end results after fabrication using 1 µL, 2 µL, or 5 µL of hysol. 1 µL kept the piezoelectric film adhered to the electrode (left). The 2 µL devices had fabrication issues when the hysol would leak out from under and create a layer of adhesion between the top electrode and glass slide (center) . The 5 µL Hysol devices had

similar failures to the 2 µL devices, but the PVDF came off of the bottom electrode (Right).

M-Mode

Motion mode (m-mode) is observing the movement of a ROI over time. The m-modes below in (**Figure 17**) are from holding a transducer over a gel pad and pressing down and then up.

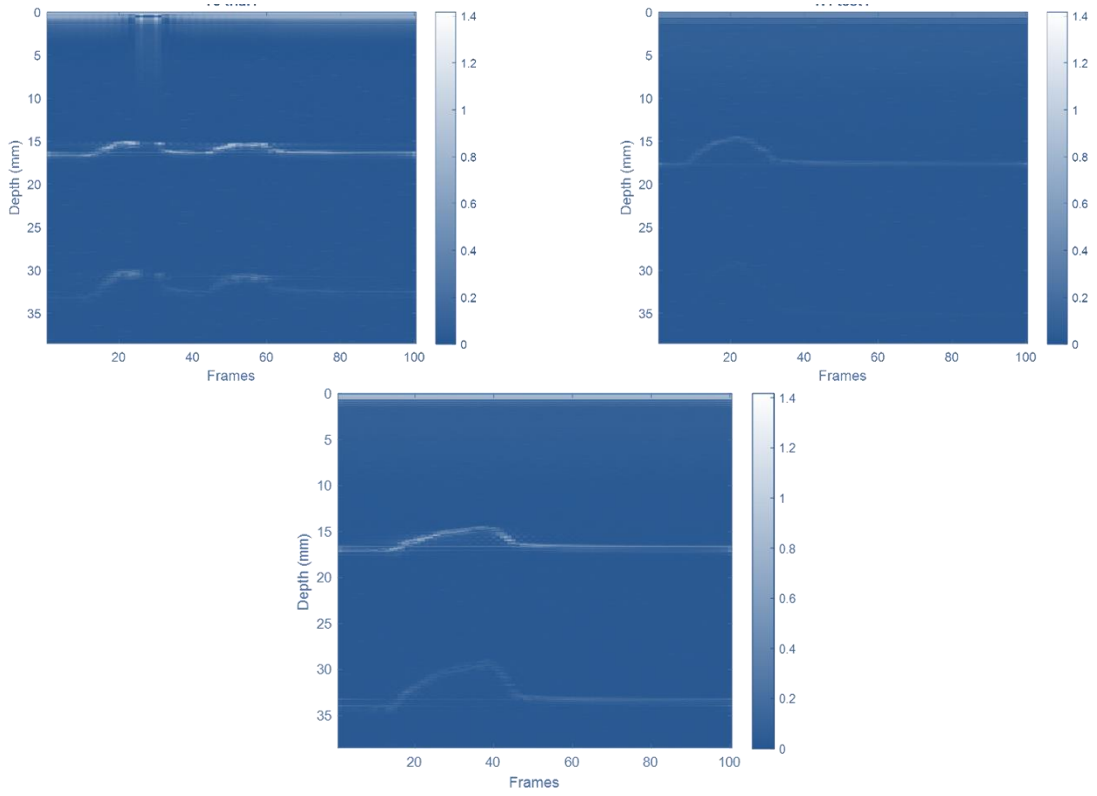

Figure 17: 1 µL of Hysol applied(Left), 2 µL of Hysol applied(center), and 5 µL of Hysol (Right). 1 µL kept the piezoelectric film adhered to the electrode (left).

The peaks in the m-mode indicate a change in depth as depth of the gel pad decreases when pushed down. The signal of the m-mode shown is in blue-scale with the

lowest pixel value being blue being the lowest pixel value of zero and white being the highest value of 1. The intensity of the signal in the image is reflective of the signal strength.

Table 8: 1 µL Hysol device, 2 µL Hysol device, and 5 µL device. The table shows the signal strength and frequency components of the transducer.

Device Name	Pulse-echo Amplitude	Center Frequency	Bandwidth
Mic1_Device 2	1.20 V	3.78 MHz	2.11 MHz
Mic2_Device 2	0.45 V	3.66 MHz	1.90 MHz
Mic5_Device 2	0.90 V	4.21 MHz	2.44 MHz

Analysis and Findings

Overall trends that were seen in all three tests suggest that a device with 5 µL is optimal for fabrication of a transducer. From the pulse-echo, there as Hysol volume decreases, signal also attenuates. The pulse-echo and hydrophone tests have similar results and show that the device with 5 µL has the approximate desired center frequency of 4 MHz and Bandwidth of 2 MHz. The hydrophone also showed the 5 µL device's ability to have an even peak pressure across the cross-section and the beam cross-section. The 5 µL device was the only device that was also able to produce an m-mode on skin. The depth is approximately 4 mm (**Figure 18)**.

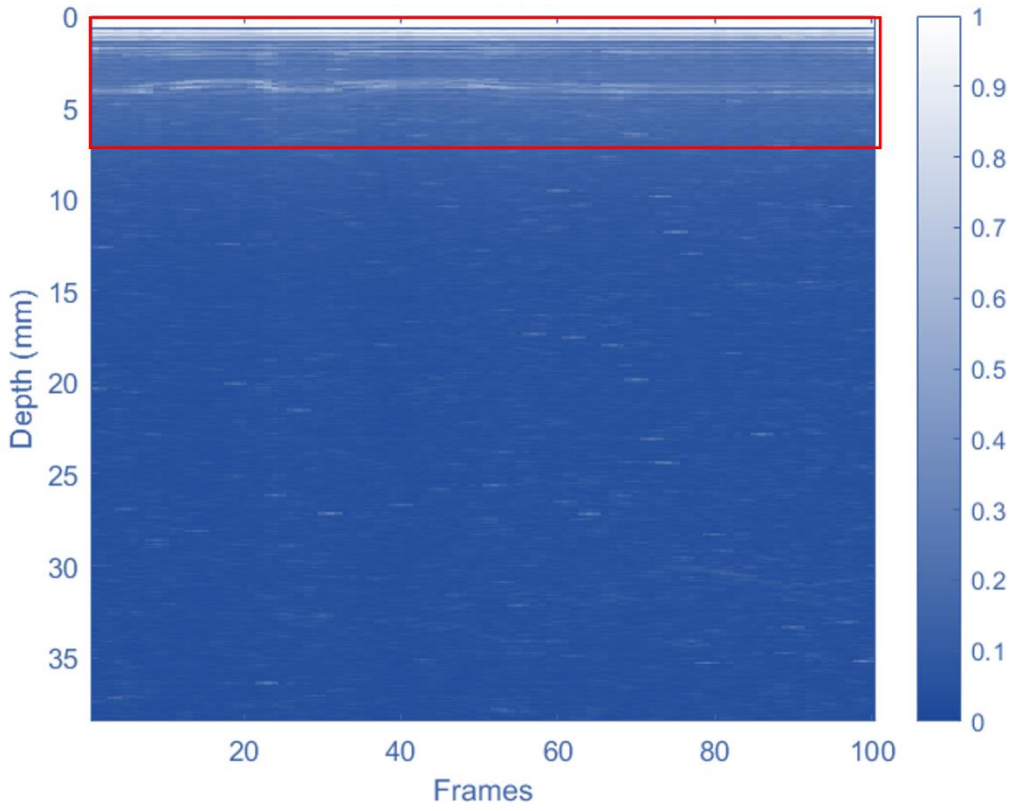

Figure 18: Device H9 is a device with 5 µL of Hysol a center frequency of 4.20 MHz and bandwidth of 2.44 MHz.

While this device penetrates through the epidermis through to subcutaneous fat and is attenuated, with proper amplification of the signal, backing layers to prevent constructive or destructive interference of the signal, and matching layer to ensure proper transmission of a signal. This device shows promise and meets the requirements for the frequency components of a device observing musculoskeletal structures.

PVDF THICKNESS EXPERIMENTS

Different Thicknesses

A transducer's piezoelectric center frequency can be calculated by knowing the thickness and speed of sound **(Eq 7)**.

$$f = \frac{v}{2d} \qquad \text{(Eq 7)}$$

If a piezoelectric material has only two electrodes, the piezoelectric material functions close to center frequency. The piezoelectric material used for the parametric experiment with the same level of Hysol and different film thicknesses of 45μm, 100 μm, or 200 μm PVDF film with electrodes purchased from PolyK. As all PVDF came with electrodes on both sides, the positive side was removed with acetone. The estimated center frequencies for the three thicknesses can be shown is the (**Table 9**).

Table 9: The table above shows the calculated center frequency for each different thickness.

Device Thickness	Center Frequency
45	24.4 MHz
100	11 MHz
200	5.5 MHz

From the calculations above, the expectation is that as the thickness increases the Center Frequency decreased. Mechanical loading may reduce the frequency response due to the Hysol adding rigidity to the piezoelectric once cured. While mechanical loading may reduce the center frequency, a downward trend in frequency response should be expected as the PVDF film increases. Thus, the purpose of testing the device with different film thicknesses is to make sure the device meets the desired center frequency, bandwidth, and acoustic pressure profile when expecting mechanical loading from other added layers on the piezoelectric material to impact the acoustic signal.

Acoustic Testing

Acoustic tests were done with a gel-pad medium and pulser-receiver for excitation of the transducer. The device was laid flat with the ground electrode side of the transducer placed on top of the device.

Table 10: Devices with 45 μm thick film

Device Name	Pulse-echo Amplitude	Center Frequency	Bandwidth
45Mic_Device1	0.80 V	6.85 MHz	7.14 MHz
45Mic_Device2	0.80 V	5.38 MHz	6.90 MHz
45Mic_Device 3	0.90 V	7.34 MHz	4.45 MHz

Table 11: Devices with 100 μm thick film

Device Name	Pulse-echo Amplitude	Center Frequency	Bandwidth
100Mic_Device1	1.30 V	3.78 MHz	2.11 MHz
100Mic_Device2	1.20 V	7.83 MHz	3.42 MHz
100Mic_Device3	0.40 V	3.42 MHz	1.89 MHz
100Mic_Device4	0.90 V	6.85 MHz	4.89 MHz
100Mic_Device5	0.40 V	5.97 MHz	3.42 MHz

Table 12: Devices with 200 μm thick film

Device Name	Pulse-echo Amplitude	Center Frequency	Bandwidth
200Mic_Device1	0.20 V	2.56 MHz	1.34 MHz
200Mic_Device2	0.40 V	1.71 MHz	1.16 MHz

The tables above have been translated into graphs below to observe trends between devices with film thicknesses of either 45 μm, 100 μm, or 200 μm. The two observations when interpreting the results for the pulse-echo tests were: 1) the change in bandwidth and 2) change in center frequency due to the different film thicknesses. When comparing the Center Frequency between the devices with different thicknesses, there was a decrease in Center Frequency as the thickness increased (**Figure 19)**. The Bandwidth was reduced as the film thickness increased (**Figure 20)**. The primary reason for focusing on these two frequency components is because the center frequency impacts the penetration depth of the image and the bandwidth impacts the resolution of the image in ultrasound. The thickness that gives a center frequency close to the desired 4MHz and

a bandwidth of 2 MHz is 100 μm PVDF film transducers. Also, the signal strength, center frequency, and bandwidth of 200 μm devices is significantly below the threshold for imaging ultrasound transducers.

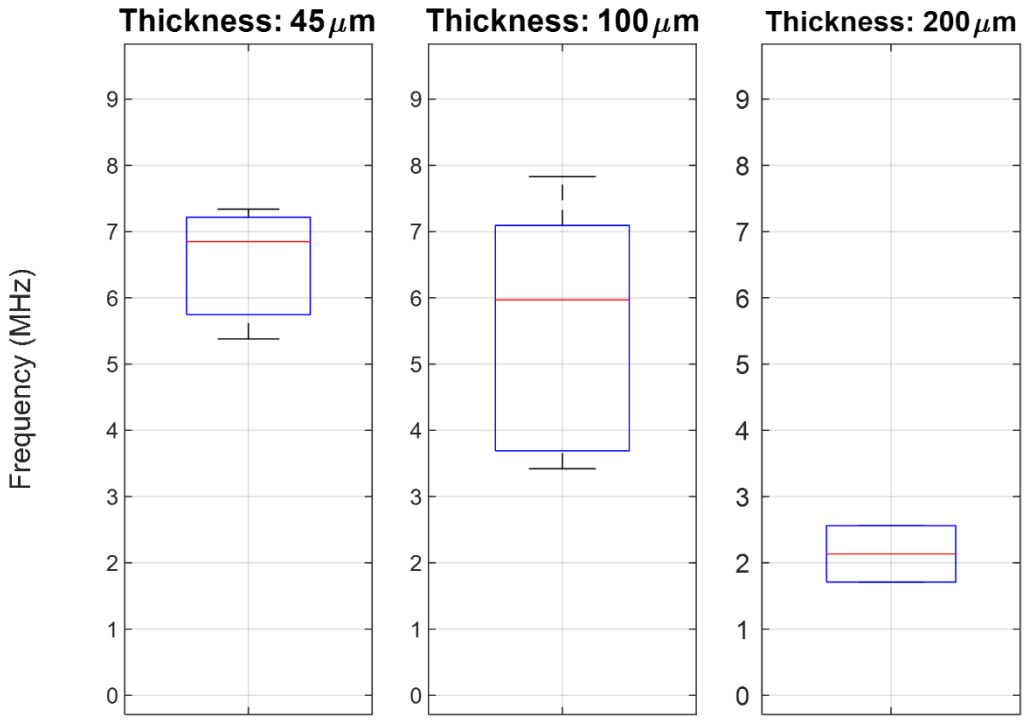

Figure 19: Comparison of the center frequencies across three different PVDF film thicknesses. As the thickness of the film increases, the center frequency decreases.

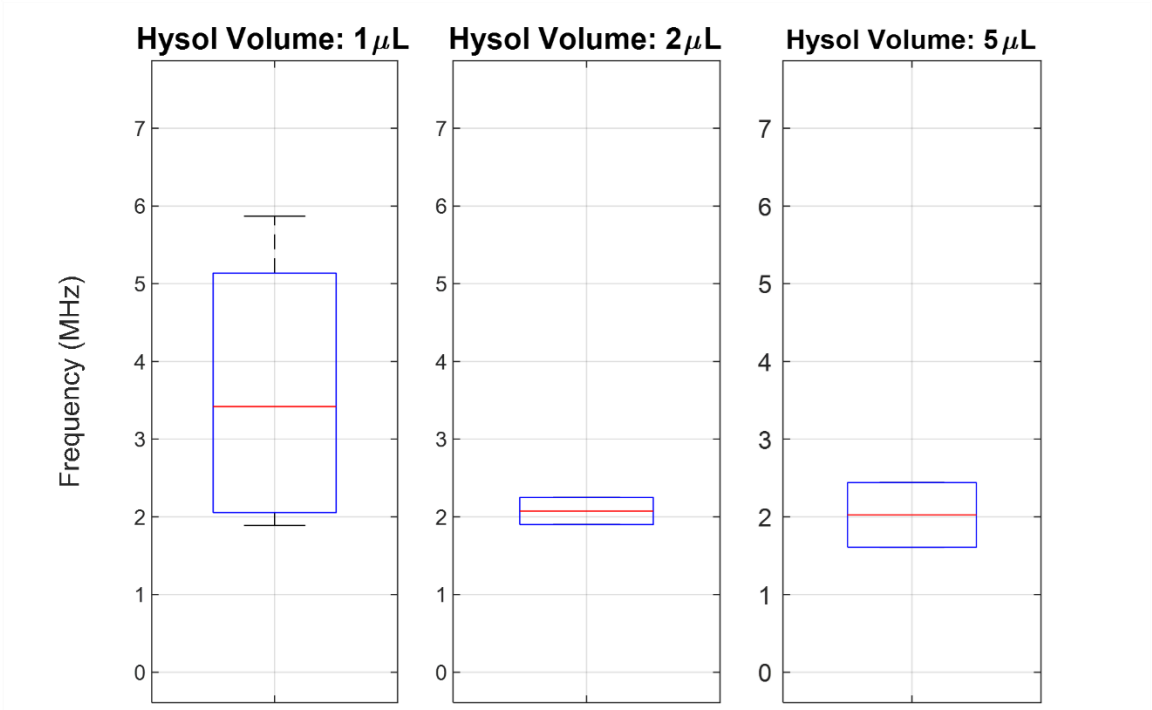

Figure 20: Comparison of the bandwidths across three different PVDF film thicknesses. As the thickness of the film increases, the bandwidth decreases.

Hydrophone Testing

Table 13: Devices that have 45 µm films

Device Name	Signal Amplitude	Center Frequency	Bandwidth
45Mic_Device1	0.16 V	8.30 MHz	2.49 MHz
45Mic_Device2	0.12 V	6.10 MHz	4.83 MHz
45Mic_Device 3	0.09 V	6.35 MHz	4.64 MHz

Table 14: Devices that have 100 µm films

Device Name	Signal Amplitude	Center Frequency	Bandwidth
100Mic_Device1	0.10 V	3.05 MHz	3.27 MHz
100Mic_Device2	0.20 V	6.35 MHz	4.81 MHz
100Mic_Device3	0.12 V	3.90 MHz	5.69 MHz

Table 15: Devices that have 200 µm films

Device Name	Signal Amplitude	Center Frequency	Bandwidth
200Mic_Device1	0.04 V	2.56 MHz	2.31 MHz

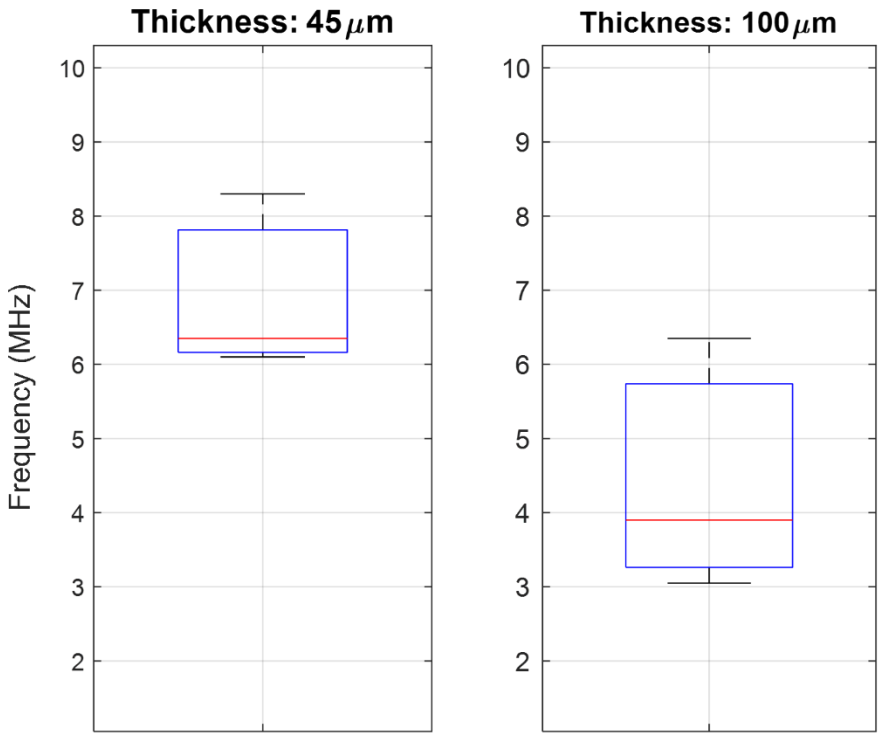

Figure 21: Chart comparing the center frequencies of different film thicknesses

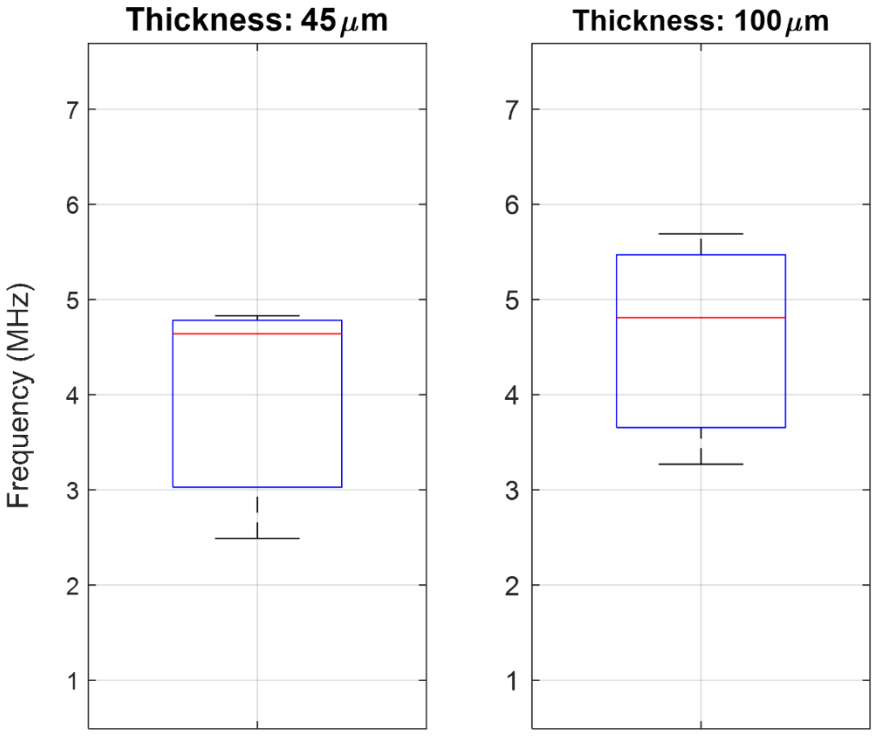

Figure 22: Chart comparing the bandwidths of different film thicknesses

From the data above there are three observations of change in center frequency, change in bandwidth, comparison to standardized frequency metrics for application, and comparison to center frequency and bandwidth of pulse-echo measurements. For the hydrophone, the center-frequency seems to decrease as thickness is increased (**Figure 21**). The Bandwidth of the device decreases as the thickness increases (**Figure 22**). The 100 μm devices have the center frequency and the bandwidth closest to the desired center frequency of 4 MHz and 2 MHz bandwidth. When comparing the Center Frequency and Bandwidth tests between both the Pulse-echo and Hydrophone tests, the devices for the 45 μm, 100 μm, 200 μm, 71 % of the devices had similar results. There is an expectation

of a small variance in bandwidth and center frequency from hydrophone data vs pulse-echo data. Variance can occur because in pulse-echo the device is both the transmitter and receiver, but in hydrophone testing the device is a transmitter and the hydrophone is the receiver of the signal (**Figure 23**). Thus, some variability is expected.

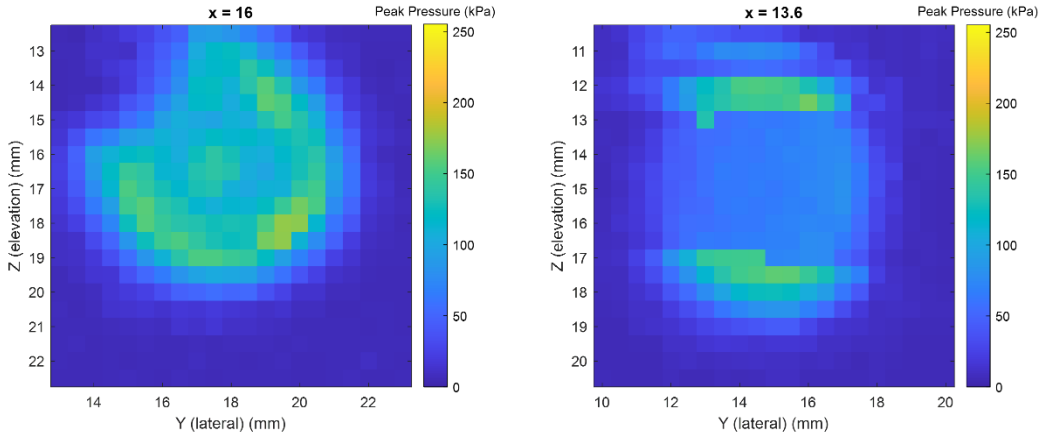

Figure 23: The devices are hydrophone scans with devices film thickness of 45 µm (left), 100 µm (center), or 200 µm (center) and a Hysol level of 1 µL

M-Mode

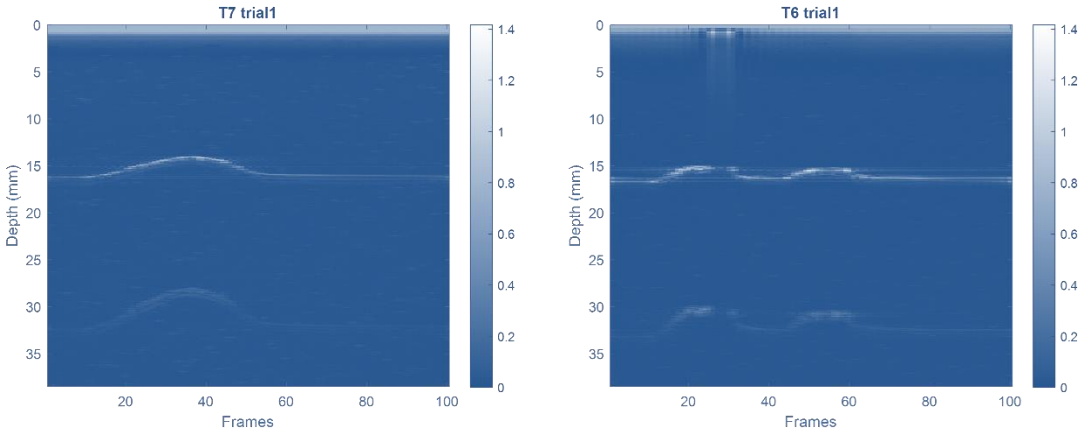

Figure 24: The devices are m-mode scans devices film thickness of 45 µm (left), 100 µm (center), or 200 µm (center) and a Hysol level of 1 µL

Analysis and Findings

Overall trends that were seen in all three tests suggest that a device with 100 is optimal for fabrication of a transducer. From the pulse-echo, there as Hysol volume decreases, signal also attenuates. The pulse-echo and hydrophone tests have similar results and show that the device with 5 µL has the approximate desired center frequency of 4 MHz and Bandwidth of 2 MHz. The hydrophone also showed the 5 µL device's ability to have an even peak pressure across the cross-section and the beam cross-section. The 5 µL device was the only device that was also able to produce an m-mode on skin (**Figure 24**). The depth is approximately 4 mm.

OPTIMAL PARAMETERS AND DISCUSSION

When observing the cross-section of the Beam profile for differing , the homogeneity of the beam profile improves as much as. The optimal parameters from the

data show that the 5 μL and 100 μm film. The only device that was able to be used for ultrasound was a device that had 5 μL of Hysol adhesive and 100 μm film. The main issues encountered through this process have been related to fabrication. Fabrication issues that may have led to inconsistencies in the beam-profile of the transducer are bubbles when mixing the two-part Hysol adhesive, gaps in between transducer and the medium the signal is propagating through, and placement of transducer on medium. Degassing the Hysol, adding an even layer of coupling gel, and optimizing the current set up to make consistent placement on the medium are all factors that can be done to optimize fabrication of the transducer. These steps have the potential to mitigate air gaps that impact the transmission of the signal. However, a device being able to show imaging through the skin does show promise of this fabrication method.

Several iterations of fabrication and optimization of fabrication were done before the experiments in this paper to determine the parametric experiments and characterization methods for the fabrication of this flexible transducer. The research in this paper lays the foundation for further exploration and fabrication of these flexible transducers. The future vision for these flexible transducers would be to integrate the transducers into a wearable systems to track muscle function during dynamic tasks. The next chapter will compare the fabricated flexible transducer against the PiezoPaint Patch and LIG-PI-PVDF composite for the application of evaluating musculoskeletal disorders.

COMPARATIVE ANALYSIS

For evaluation of MSKIs, several strategies are being used to fabricate flexible transducers. A flexible transducer alone attached to a bulky ultrasound system can impact our observations of our understanding of muscle function during dynamic tasks. Ideally, a portable system in combination with a flexible transducer would allow observation of muscle function during dynamic tasks. The next chapter will compare the fabricated flexible transducer against the PiezoPaint Patch and LIG-PI-PVDF composite for the application of evaluating musculoskeletal disorders.

COMPARISON BETWEEN THREE DEVICES

Three options of flexible transducers in consideration of being integrated into wearable systems are the Piezopaint Patch, Graphene-PI-PVDF composites, and the flexible transducers discussed in previous chapters. The Piezopaint Patch is a piezoelectric ink is a device with the bottom electrode screen printed onto the on a flexible PET substrate and the Piezopaint is interposed between two electrodes (**Figure 25**).

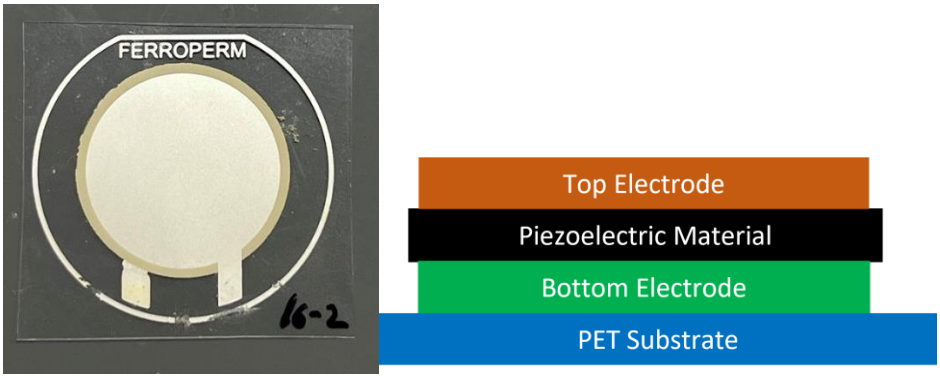

Figure 25: Front-view (left) and cross-sectional view (right) Piezopaint Transducer

The Piezopaint Patch is a product that is manufactured by a industry specialist using a industry standard material of PZT for ultrasound transducers in the form of a proprietary ink. The benefit of this patch is that it uses an industry standard material for ultrasound transducers that is known to perform well.

Another method pursued by The Kang Group is Graphene-PI-PVDF composites where the Graphene-PI-PVDF composites are transducers that have a PVDF with a ground electrode on one side and a Polyimide(PI) tape on the other side (**Figure 26**).

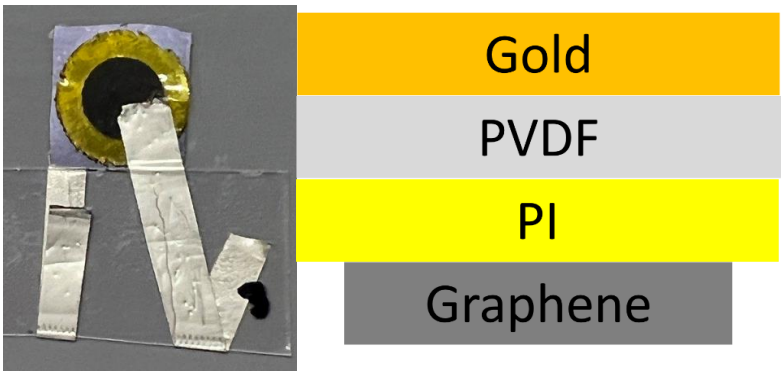

Figure 26: Front-view (left) and cross-sectional view (right) the Graphene-PI-PVDF composites

The side of the PI not in contact with the PVDF is graphitized through laser-induced graphitization. Laser induced graphitization is done through using a CAD software where the electrode can be designed and modified in minutes. The benefits of this method are that the positive electrode dimensions and design are both customizable the method mitigates having the variability in adhesion of the layers as seen in the device fabricated in earlier chapters. This chapter will go over the performance of the Piezopaint Patch, the Kang Group composites, and perform a comparative analysis against the fabricated flexible transducer in previous chapters.

Acoustic Testing

The acoustic testing is done similarly to previous chapters with the following settings and set-up:

Table 16: Settings for pulser-receiver

Pulse-Echo Setting	Setting Value
PRF	1000 Hz
Energy	4 (16 μ J)
Damping	1 (12 Ohms)
Gain	39 dB
High Pass Filter	OFF
Low Pass Filter	ON

The tables above have been translated into graphs below to observe trends between the piezopaint device, the Graphene-PI-PVDF composites and the optimal flexible transducer

device. The two observations when interpreting the results for the pulse-echo tests were: 1) the change in bandwidth and 2) change in center frequency of each device.

Table 17: Results of metrics to evaluate all devices pulse-echo test

Device Name	Pulse-echo Amplitude	Center Frequency	Bandwidth
PiezoPaint	2.00 V	3.85 MHz	0.67 MHz
Flex_Device	0.90 V	4.21 MHz	2.44 MHz
Graphene_1	0.15 V	8.30 MHz	4.40 MHz
Graphene_2	0.20 V	8.81 MHz	5.38 MHz

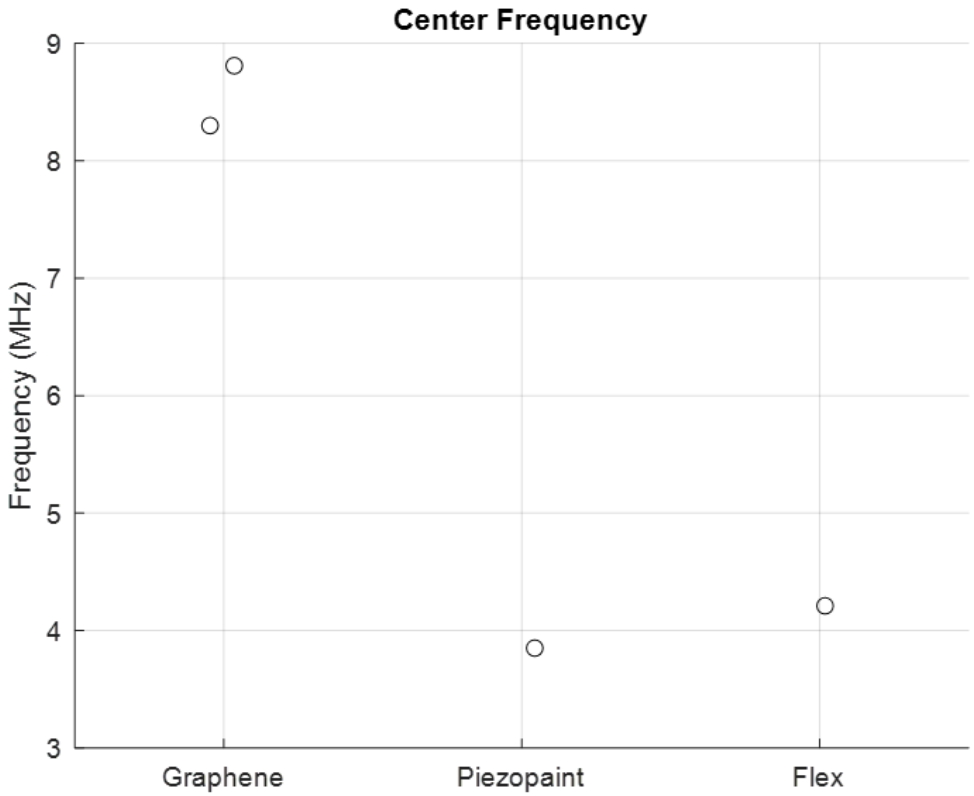

Figure 27: Comparison of Center Frequencies between devices

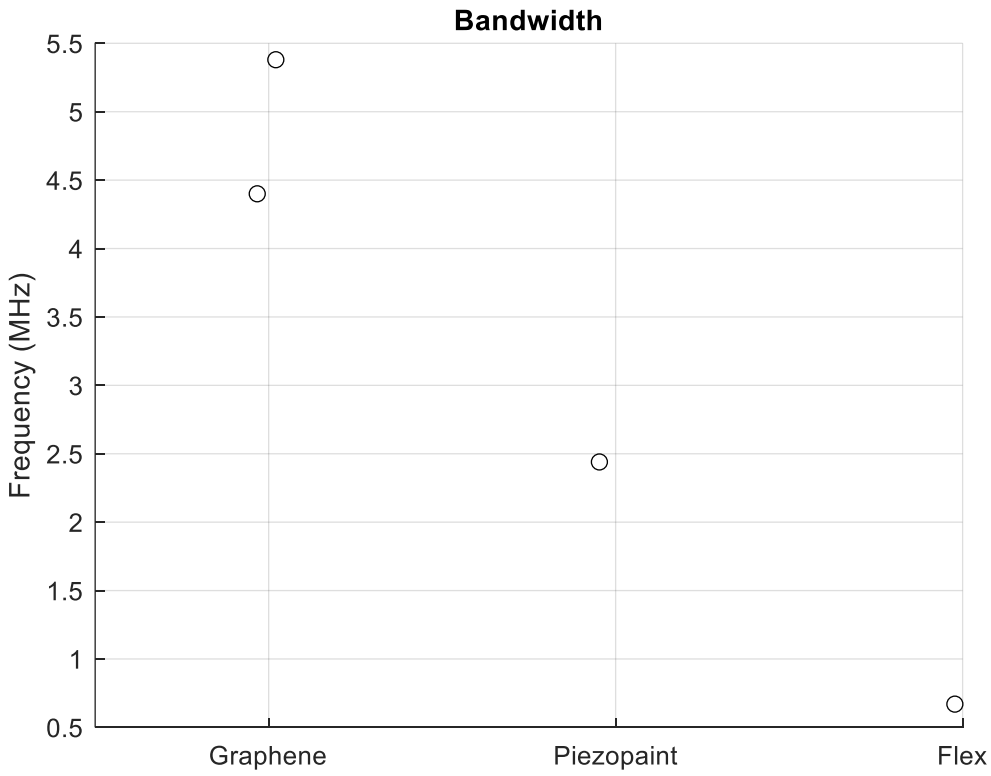

Figure 28: Comparison of Bandwidths between devices

The Graphene-PI-PVDF has the highest average frequency at 8.55 MHz, the flexible fabricated transducer(H9) has 4.21 MHz, and the Piezopaint has the lowest center frequency at 3.85 MHz (**Figure 27**). The Graphene-PI-PVDF have the highest average bandwidth at 5 MHz, the flexible fabricated transducer(H9) a bandwidth of 2.44 MHz, and the Piezopaint has the lowest bandwidth at 0.67 MHz (**Figure 28)**. Conclusions that can be drawn from pulse-echo testing based on the frequency components of the signal of the Graphene-PI-PVDF the device will have the best resolution, low penetration depth, and weakest signal due to the high center frequency, wide bandwidth, and low signal

amplitude. Piezopaint will have the worst resolution, high penetration depth, and the strongest signal due to the low center frequency, narrow bandwidth, and high signal amplitude. The fabricated flexible transducer discussed in earlier chapters will have the moderate resolution, moderate penetration depth, and moderate signal due to the low center frequency, wide bandwidth, and moderate signal amplitude. Based on the pulse-echo results application of imaging at 4MHz with a Bandwidth of 2 MHz, the most ideal device would be either the fabricated flexible transducer discussed in earlier chapters or the Piezopaint transducer.

Hydrophone Testing

Table 18: Hydrophone results of metrics to evaluate all devices

Device Name	Signal Amplitude	Center Frequency	Bandwidth
PiezoPaint	0.10 V	3.54 MHz	1.00 MHz
Flex_Device	0.06 V	3.66 MHz	2.05 MHz
Graphene_1	0.06 V	8.30 MHz	8.40 MHz
Graphene_2	0.02 V	9.64 MHz	4.24 MHz

The Graphene-PI-PVDF have the highest average frequency at 8.97 MHz, the flexible fabricated transducer(H9) has 3.66 MHz, and the Piezopaint has the lowest center frequency at 3.54 MHz . The Graphene-PI-PVDF have the highest average bandwidth at 6.3 MHz, the flexible fabricated transducer(H9) a bandwidth of 2.05 MHz, and the

Piezopaint has the lowest bandwidth at 1.00 MHz (**Table 18)**. Conclusions that can be drawn from pulse-echo testing based on the frequency components of the signal of the Graphene-PI-PVDF the device will have the best resolution, low penetration depth, and weakest signal due to the high center frequency, wide bandwidth, and low signal amplitude. Piezopaint will have a will have the worst resolution, high penetration depth, and the strongest signal due to the low center frequency, narrow bandwidth, and high signal amplitude. The fabricated flexible transducer discussed in earlier chapters will have the moderate resolution, moderate penetration depth, and moderate signal due to the low center frequency, wide bandwidth, and moderate signal amplitude. Based on the pulse-echo results application of imaging at 4MHz with a Bandwidth of 2 MHz, the most ideal device would be either the fabricated flexible transducer discussed in earlier chapters or the Piezopaint transducer. All three devices have an even beam profile that spans 40 mm.

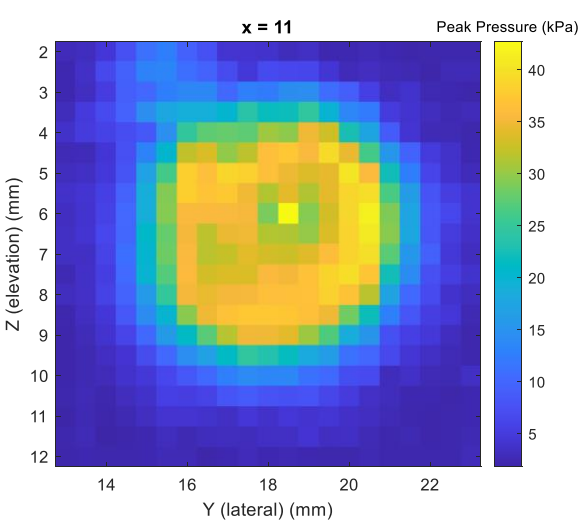

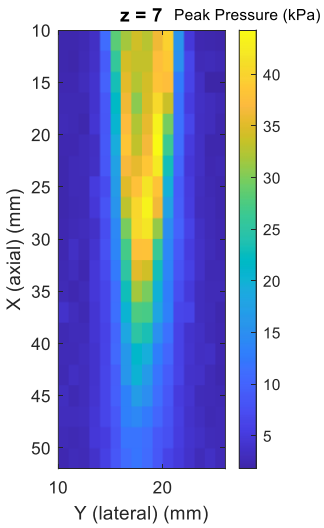

Figure 29: Hydrophone scan cross-sectional view(left) and axial view (right) of fabricated flexible transducer discussed in previous chapters

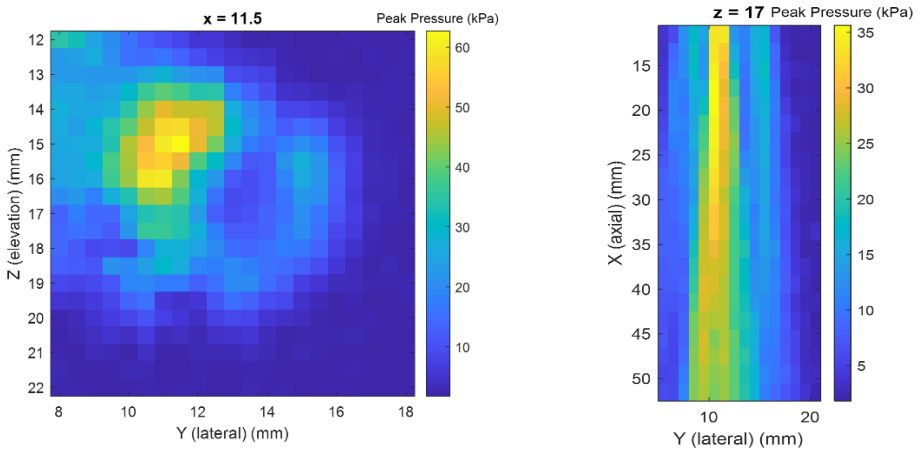

Figure 30: Hydrophone scan cross-sectional view(left) and axial view (right) of Graphene-PI-PVDF composite

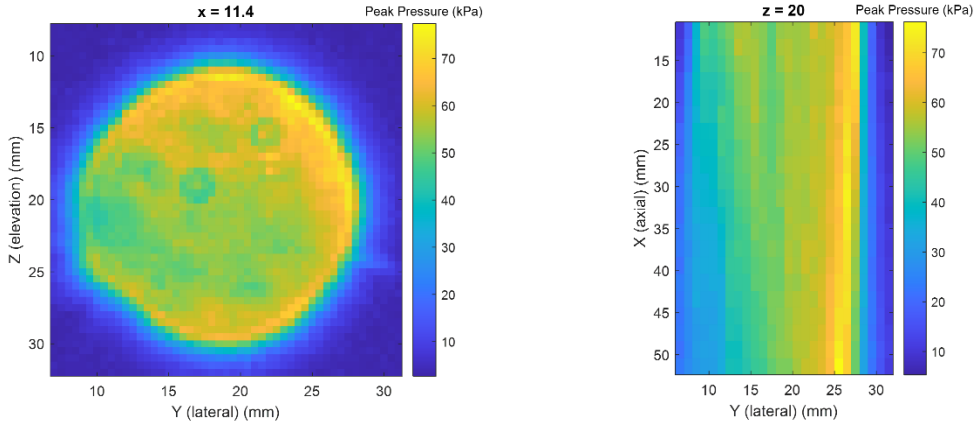

Figure 31: Hydrophone scan cross-sectional view(left) and axial view (right) of Piezopaint Transducer

The Piezopaint has highest pressure is 60 kPa (**Figure 31**). The Graphene-PI-PVDF the device has a peak pressure of 10 kPa (**Figure 30**). The flexible transducer has a peak pressure of 50 kPa (**Figure 29**). The Graphene-PI-PVDF composites have a

average peak pressure of 20 kPa. Thus, the Piezopaint or the flexible transducer would be the best for the application of observing muscle function and MSKIs.

M-Mode

When looking at an m-mode characteristics to look for are signal strength resolution, and penetration depth. The signal strength of an m-mode is determined by the intensity of the line. The resolution is dependent on the variation and smoothness of the signal. The penetration depth determines how deep is the imaging ability. Piezopaint has the strongest signal strength based on the thickness, worse resolution, and the deepest penetration depth (**Figure 32**).

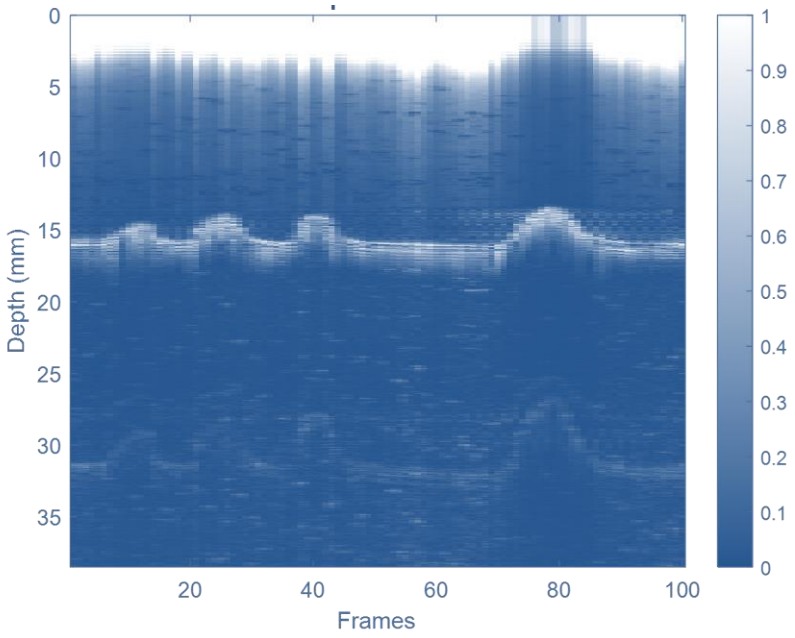

Figure 32: M-mode of Piezopaint

The Graphene-PI-PVDF has a low signal strength, a higher resolution, and the shortest penetration depth (**Figure 33 , 34**). The flexible transducer mentioned in previous chapters had the half the signal strength of the Piezopaint based on the amplitude of the signal, had better resolution based on the wide bandwidth, and had the same depth perception as the Piezopaint (**Figure 35**). Thus, the Piezopaint or the flexible transducer would be the best for the application of observing muscle function and MSKIs.

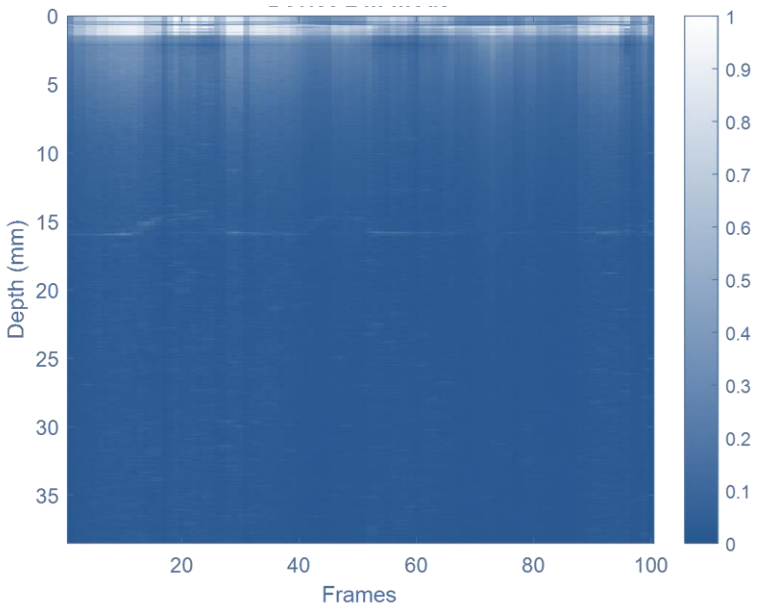

Figure 33: M-mode of Graphene-PI-PVDF Transfer Device 2

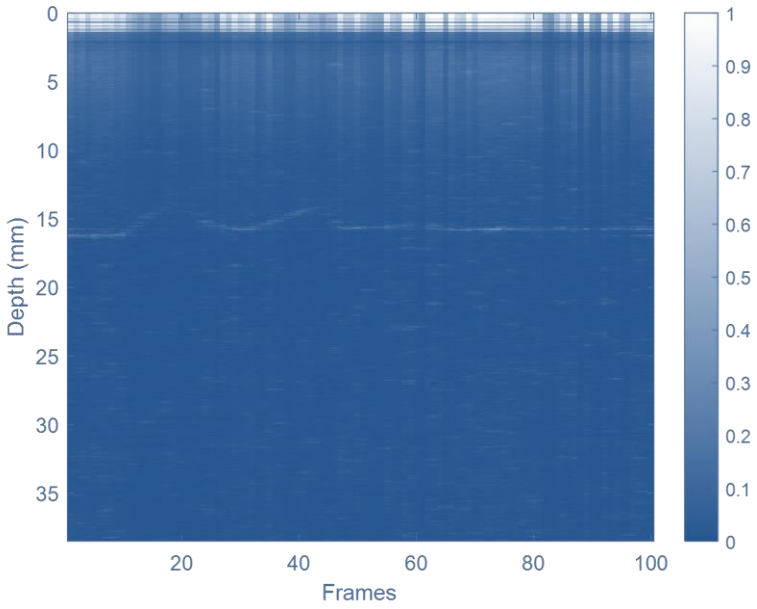

Figure 34: M-mode of Graphene-PI-PVDF Transfer Device 3

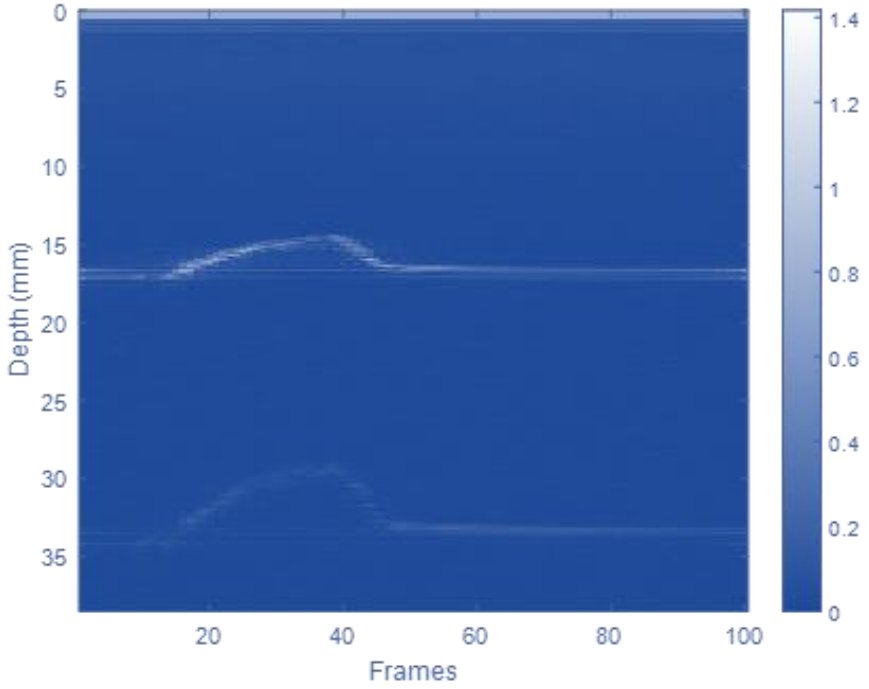

Figure 35: M-mode of flexible transducer discussed in earlier chapters

FUTURE WORK

LIMITATIONS AND FUTURE WORK

The flexible transducer discussed in previous chapters and the Piezopaint transducer frequency components matched literature for imaging musculoskeletal structures with a center frequency of 4 MHz and Bandwidth of 2 MHz, had an even beam profile, and were able to image about 3.5 cm in depth.

While the flexible transducer discussed in previous chapters and the Piezopaint transducer shows promise, there are a few improvements that can be made. Both devices could be improved by adding a matching and backing layer. A matching layer is a layer between the transducer and tissue that allows for better transmission of the signal by reducing the acoustic impedance between the transducer and tissue. A backing layer could also be added to increase the bandwidth of the device as improving the bandwidth will improve the resolution [40]. On top of the fabrication methods being improved, increasing the data size can also be done in future studies to observe fabrication and transducer performance variability.

This work shows promise for two types of transducer fabrication methods and can be seen as building the foundation of the flexible transducer that can eventually be integrated into wearable systems to observe and diagnose MSKIs.

REFERENCES

[1] The National Safety Council, "Work Safety: Musculoskeletal Injuries and Illnesses," Injury Facts, 2021. https://injuryfacts.nsc.org/work/safety-topics/musculoskeletal-injuries/ (accessed Jul. 06, 2023).

[2] C. Mokri, M. Bamdad, and V. Abolghasemi, "Muscle force estimation from lower limb EMG signals using novel optimised machine learning techniques," Medical & Biological Engineering & Computing, vol. 60, no. 689–699, Jan. 2022, doi: https://doi.org/10.1007/s11517-021-02466-z.

[3] S. Weinstein, E. Yelin, L. Callahan, K. Shea, and The Burden of Musculoskeletal Diseases in the United States: Prevalence, Societal and Economic Costs (BMUS), "BMUS: The Burden of Musculoskeletal Diseases in the United States," BMUS: The Burden of Musculoskeletal Diseases in the United States, 2012. https://www.boneandjointburden.org/ (accessed Jul. 06, 2023).

[4] Cleveland Clinic, "Musculoskeletal Pain | Cleveland Clinic," Cleveland Clinic, 2014. https://my.clevelandclinic.org/health/diseases/14526-musculoskeletal-pain (accessed Jul. 06, 2023).

[5] C. N. Riggin, T. R. Morris, and L. J. Soslowsky, Tendinopathy II. Academic Press, 2015, pp. 149–183. doi: https://doi.org/10.1016/b978-0-12-801590-2.00005-3.

[6] H. J. Woodford and C. I. Price, "EMG biofeedback for the recovery of motor function after stroke," Cochrane Database of Systematic Reviews, vol. 2010, no. 1, Apr.

2007, doi: https://doi.org/10.1002/14651858.cd004585.pub2.

[7] S. Dosen, M. Markovic, K. Somer, B. Graimann, and D. Farina, “EMG Biofeedback for online predictive control of grasping force in a myoelectric prosthesis,” Journal of NeuroEngineering and Rehabilitation, vol. 12, no. 1, Jun. 2015, doi: https://doi.org/10.1186/s12984-015-0047-z.

[8] Chippewa Valley Technical College, E. Christman, K. Ernstmeyer, and Open RN, Nursing Skills, 13.4 Musculoskeletal Assessment., vol. 13.4. Ann Arbor, Michigan: Xanedu Publishing Inc, 2021. Accessed: Jul. 06, 2023. [Online]. Available: https://wtcs.pressbooks.pub/nursingskills/chapter/13-4-musculoskeletal-assessment/

[9] Yale Medicine, “Musculoskeletal Ultrasound,” Yale Medicine, Nov. 11, 2019. https://www.yalemedicine.org/conditions/musculoskeletal-ultrasound (accessed Jul. 06, 2023).

[10] ScienceDirect, “Dynamometer - an overview | ScienceDirect Topics,” www.sciencedirect.com, Jun. 07, 2021. https://www.sciencedirect.com/topics/nursing-and-health-professions/dynamometer (accessed Jul. 06, 2023).

[11] R. Subbu, R. Weiler, and G. Whyte, “The practical use of surface electromyography during running: does the evidence support the hype? A narrative review,” BMJ Open Sport & Exercise Medicine, vol. 1, no. 1, p. e000026, Dec. 2015, doi: https://doi.org/10.1136/bmjsem-2015-000026.

[12] R. Chowdhury, M. Reaz, M. Ali, A. Bakar, K. Chellappan, and T. Chang, “Surface Electromyography Signal Processing and Classification Techniques,” Sensors, vol. 13, no. 9, pp. 12431–12466, Sep. 2013, doi: https://doi.org/10.3390/s130912431.

[13] R. Merletti, I. Campanini, W. Z. Rymer, and C. Disselhorst-Klug, “Editorial: Surface Electromyography: Barriers Limiting Widespread Use of sEMG in Clinical Assessment and Neurorehabilitation,” Frontiers in Neurology, no. 12, Feb. 2021, doi: https://doi.org/10.3389/fneur.2021.642257.

[14] M. P, M. R, H. S, G. M, and K. W, “A Systematic Review of Dynamometry and its Role in Hand Trauma Assessment,” The Open Orthopaedics Journal, vol. 6, no. 1, pp. 95–102, Feb. 2012, doi: https://doi.org/10.2174/1874325001206010095.

[15] A. Pinto et al., “Sources of error in emergency ultrasonography,” Critical Ultrasound Journal, vol. 5, no. S1, Jul. 2013, doi: https://doi.org/10.1186/2036-7902-5-s1-s1.

[16] X. Zhu, H. Hu, S. Sternini, S. Xy, and F. Lanza Di Scalea, “Stretchable Ultrasonic Transducer Arrays for Three-Dimensional Imaging on Complex Surfaces,” in Conference: Structural Health Monitoring 2019, Structural Health Monitoring, Nov. 2019. Accessed: Jul. 06, 2023. [Online]. Available: https://www.dpi-proceedings.com/index.php/shm2019/article/view/32341

[17] R. van Schaijk, “CMUT and PMUT: New Technology Platform for Medical Ultrasound Rob Van Schaijk,” Philips Engineering Solutions, Nov. 2018. Accessed: Jul. 06, 2023. [Online]. Available: https://www.engineeringsolutions.philips.com/app/uploads/2019/03/CMUT-and-PMUT-Rob-van-Schaijk-November-2018.pdf

[18] M. Habib, I. Lantgios, and K. Hornbostel, “A Review of ceramic, Polymer and

Composite Piezoelectric Materials," Journal of Physics D: Applied Physics, vol. 55, no. 42, p. 423002, Aug. 2022, doi: https://doi.org/10.1088/1361-6463/ac8687.

[19] D.-M. Shin, S. W. Hong, and Y.-H. Hwang, "Recent Advances in Organic Piezoelectric Biomaterials for Energy and Biomedical Applications," Nanomaterials, vol. 10, no. 1, p. 123, Jan. 2020, doi: https://doi.org/10.3390/nano10010123.

[20] H. Wang and A. Jasim, "Piezoelectric energy harvesting from pavement," Eco-Efficient Pavement Construction Materials, pp. 367–382, Jan. 2020, doi: https://doi.org/10.1016/B978-0-12-818981-8.00014-X.

[21] ScienceDirect, "Piezoelectric Material - an overview | ScienceDirect Topics," www.sciencedirect.com, Feb. 24, 2020. https://www.sciencedirect.com/topics/engineering/piezoelectric-material (accessed Jul. 02, 2022).

[22] Q. Zhou, K. H. Lam, H. Zheng, W. Qiu, and K. K. Shung, "Piezoelectric Single Crystal Ultrasonic Transducers for Biomedical Applications," Progress in Materials Science, vol. 66, pp. 87–111, Oct. 2014, doi: https://doi.org/10.1016/j.pmatsci.2014.06.001.

[23] S. A. Pullano, C. D. Critello, M. G. Bianco, M. Menniti, and A. S. Fiorillo, "PVDF Ultrasonic Sensors for In-Air Applications: a Review," IEEE Transactions on Ultrasonics, Ferroelectrics, and Frequency Control, vol. 68, no. 7, pp. 2324–2335, Jul. 2021, doi: https://doi.org/10.1109/tuffc.2021.3078069.

[24] Torben Marhenke, S. J. Sanabria, Bhaskara Rao Chintada, R. Furrer, J. Neuenschwander, and S. Shimizu, "Acoustic Field Characterization of Medical Array Transducers Based on Unfocused Transmits and Single-Plane Hydrophone

Measurements," Sensors, vol. 19, no. 4, pp. 863–863, Feb. 2019, doi: https://doi.org/10.3390/s19040863.

[25] M. S. Haynes, S. Verweij, M. Moghaddam, and P. L. Carson, "Self-characterization of Commercial Ultrasound Probes in Transmission Acoustic Inverse scattering: Transducer Model and Volume Integral Formulation," IEEE Transactions on Ultrasonics, Ferroelectrics, and Frequency Control, vol. 61, no. 3, pp. 467–480, Mar. 2014, doi: https://doi.org/10.1109/tuffc.2014.2931.

[26] D. Neumann and E. Kollorz, "Ultrasound," Medical Imaging Systems, pp. 237–249, Jan. 2018, doi: https://doi.org/10.1007/978-3-319-96520-8_11.

[27] K. Zhu et al., "Enhancement of Ultrasonic Transducer Bandwidth by Acoustic Impedance Gradient Matching Layer," Sensors (Basel), vol. 22, no. 20, pp. 8025–8025, Oct. 2022, doi: https://doi.org/10.3390/s22208025.

[28] S. Grogan, C. Mount, StatPearls Publishing, and Treasure Island (FL), "Ultrasound Physics and Instrumentation," Ultrasound Physics and Instrumentation, Jan. 2023, Accessed: Jul. 22, 2023. [Online]. Available: https://www.ncbi.nlm.nih.gov/books/NBK570593/

[29] Ibrahim AlMohimeed and Y. Ono, "Flexible and Wearable Ultrasonic Sensor for Assessment of Skeletal Muscle Contractile Properties," 2019 IEEE International Conference on Flexible and Printable Sensors and Systems (FLEPS), Jul. 2019, doi: https://doi.org/10.1109/fleps.2019.8792301.

[30] R. A. Goes et al., "Musculoskeletal Injuries in Athletes from Five modalities: a cross-sectional Study," BMC Musculoskeletal Disorders, vol. 21, no. 1, Feb. 2020, doi: https://doi.org/10.1186/s12891-020-3141-8.

[31] T.-T. Chang, Q. Yang, P. Chen, and X. Wang, “Epidemiology of Musculoskeletal Injuries in the Navy: a Systematic Review,” Int J Public Health, vol. 67, Dec. 2022, doi: https://doi.org/10.3389/ijph.2022.1605435.

[32] S. Sanchez, T. Arlata, S. Arshad, S. Cheng, A. Saunders, and University of Texas Medical Branch, “Musculoskeletal Injuries,” www.utmb.edu, Aug. 24, 2022. https://www.utmb.edu/pedi_ed/CoreV2/Musculoskeletal/Musculoskeletal_print.html (accessed Jul. 22, 2023).

[33] P. H. Lento and S. Primack, “Advances and Utility of Diagnostic Ultrasound in Musculoskeletal Medicine,” Current Reviews in Musculoskeletal Medicine, vol. 1, no. 1, pp. 24–31, Nov. 2007, doi: https://doi.org/10.1007/s12178-007-9002-3.

[34] Z. Czyrny, “Standards for musculoskeletal ultrasound,” Journal of Ultrasonography, vol. 17, no. 70, pp. 182–187, Sep. 2017, doi: https://doi.org/10.15557/jou.2017.0027.

[35] S. Bianchi and C. Martinoli, Ultrasound of the Musculoskeletal System. Berlin, Heidelberg: Springer Berlin Heidelberg, 2007. doi: https://doi.org/10.1007/978-3-540-28163-4.

[36] S. Butler, “Properties of Transducers: Underwater Sound Sources and Receivers,” apps.dtic.mil, Dec. 19, 2018. https://apps.dtic.mil/sti/citations/AD1068326 (accessed Jul. 22, 2023).

[37] A. Goldstein and R. L. Powis, “Medical Ultrasonic Diagnostics,” Ultrasonic

Instruments and Devices I - Reference for Modem Instrumentation, Techniques, and Technology, vol. 23, no. 2, pp. 43–195, 1999, doi: https://doi.org/10.1016/s0893-388x(99)80012-8.

[38] S. Kulkarni, “Frequency Domain and Fourier Transforms,” Princeton University, 2000. Accessed: Jul. 22, 2023. [Online]. Available: https://www.princeton.edu/~cuff/ele201/kulkarni_text/frequency.pdf

[39] Onda Corporation, “Onda Hydrophone Handbook,” www.ondacorp.com, Feb. 2023. https://www.ondacorp.com/Handbook/mobile/index.html#p=1 (accessed Jul. 06, 2023).

[40] International Atomic Energy Agency, Diagnostic radiology physics : a handbook for teachers and students. Vienna: Intl Atomic Energy Agency, 2013. Accessed: Jul. 06, 2023. [Online]. Available: https://humanhealth.iaea.org/HHW/MedicalPhysics/TheMedicalPhysicist/Studentscorner/HandbookforTeachersandStudents/

[41] D. Giraud and B. Nazer, “A Rapid Method for pressure-mapping Ultrasound Fields Using a Moving Hydrophone,” Journal of the Acoustical Society of America, vol. 150, no. 4_Supplement, pp. A55–A55, Oct. 2021, doi: https://doi.org/10.1121/10.0007606.

[42] M. T. Burgess and E. E. Konofagou, “Fast Qualitative two-dimensional Mapping of Ultrasound Fields with Acoustic cavitation-enhanced Ultrasound Imaging,” The Journal of the Acoustical Society of America, vol. 146, no. 2, pp. EL158–EL164, Aug. 2019, doi: https://doi.org/10.1121/1.5122194.

[43] P. Beard, “Biomedical Photoacoustic Imaging,” Interface Focus, vol. 1, no. 4, pp. 602–631, Jun. 2011, doi: https://doi.org/10.1098/rsfs.2011.0028.

[44] Radiology Key , “Ultrasound Physics,” Radiology Key, May 20, 2019. https://radiologykey.com/ultrasound-physics-2/ (accessed Jun. 06, 2023).

[45] Voltera Inc., “NOVA - A Flexible and Printed Electronics Platform | Voltera,” Voltera Inc. https://www.voltera.io/nova (accessed Jul. 06, 2023).

[46] J. Seibert, “Physics of Ultrasound,” Lippincott Williams & Wilkins, Dec. 2011. Accessed: Jul. 22, 2023. [Online]. Available: https://eu-ireland-custom-media-prod.s3-eu-west-1.amazonaws.com/UKMEAEU/eSample/22-01/9780323596428.pdf

[47] S. Sikdar, Q. Wei, and N. Cortes, “Dynamic Ultrasound Imaging Applications to Quantify Musculoskeletal Function,” Exercise and Sport Sciences Reviews, vol. 42, no. 3, pp. 126–135, Jul. 2014, doi: https://doi.org/10.1249/jes.0000000000000015.

[48] J. E. Brandenburg et al., “Ultrasound Elastography: the New Frontier in Direct Measurement of Muscle Stiffness,” Archives of Physical Medicine and Rehabilitation, vol. 95, no. 11, pp. 2207–2219, Nov. 2014, doi: https://doi.org/10.1016/j.apmr.2014.07.007.

[49] ScienceDirect , “Hysol - an Overview | ScienceDirect Topics,” www.sciencedirect.com, Nov. 18, 2022. https://www.sciencedirect.com/topics/engineering/hysol (accessed Jul. 22, 2023).

[50] ScienceDirect , “Polyethylene Terephthalate - an Overview | ScienceDirect Topics,” Sciencedirect.com, 2017. https://www.sciencedirect.com/topics/earth-and-planetary-sciences/polyethylene-terephthalate (accessed Jul. 06, 2023).

[51] Z. He et al., “Simultaneous Enhancement of Open-Circuit Voltage, Short-Circuit

Current Density, and Fill Factor in Polymer Solar Cells," Advanced Materials, vol. 23, no. 40, pp. 4636–4643, Sep. 2011, doi: https://doi.org/10.1002/adma.201103006.

[52] Iowa State University Center for Nondestructive Evaluation, "Nondestructive Evaluation Techniques : Ultrasound," www.nde-ed.org, 2021. https://www.nde-ed.org/NDETechniques/Ultrasonics/ultrasonicFormula.xhtml (accessed Jun. 06, 2023).

[53] D. Callens, C. Bruneel, and J. Assaad, "Matching Ultrasonic Transducer Using Two Matching Layers Where One of Them Is Glue," NDT & E International, vol. 37, no. 8, pp. 591–596, Dec. 2004, doi: https://doi.org/10.1016/j.ndteint.2004.03.005.

BIOGRAPHY

Antarjot Kaur received her Bachelor of Science in Bioengineering from George Mason University in 2021, After receiving her Master of Science in Bioengineering from George Mason University in 2023, she will pursue her PhD at Virginia Polytechnic Institute and State University.